Dissociating stimulus encoding and task demands in ECoG responses from human visual cortex

Zeeshan Qadir[1,2], Harvey Huang[3], Müge Özker[4†], Daniel Yoshor[4‡], Michael S. Beauchamp[4‡], Kendrick Kay[5*], Dora Hermes[2*]

***For correspondence:** hermes.dora@mayo.edu (DH); kay@umn.edu (KK); (These authors contributed equally to this work)

Present address: †Neurobiology of Language Department, Max Plank Inst for Psycholinguistics, Netherlands; ‡Department of Neurosurgery, Perelman School of Medicine, University of Pennsylvania, PA, USA

[1]Graduate School of Biomedical Sciences, Mayo Clinic, Rochester, United States; [2]Department of Physiology and Biomedical Engineering, Mayo Clinic, Rochester, United States; [3]Medical Scientist Training Program, Mayo Clinic, Rochester, United States; [4]Department of Neurosurgery, Baylor College of Medicine, Houston, United States; [5]Center for Magnetic Resonance Research, Dept of Radiology, University of Minnesota, Minneapolis, United States

Abstract

Brain responses to sensory stimuli depend on the specific task performed by the observer. Previously, fMRI measurements in ventral temporal cortex (VTC) showed that BOLD responses to words and faces scale with the difficulty of a categorization task compared to responses observed during a fixation task (***Kay and Yeatman, 2017***). This scaling of BOLD responses is thought to be driven by the engagement of cognitive functions during image categorization. To understand how these cognitive task demands change dynamically over time and influence neural activity in VTC, we measured electrocorticography (ECoG) data in two human participants during the same experimental tasks. The ECoG high frequency broadband activity (>70 Hz) showed that local neuronal responses increased with image contrast (as expected for sensory encoding) and were scaled by task demands 0.2 seconds after stimulus onset. In contrast, ECoG low frequency activity in the alpha/beta range (8-28 Hz) was insensitive to image contrast and showed larger suppression with increasing task demands. These results indicate that high frequencies in VTC reflect both the encoding of sensory inputs and task demands, similar to prior BOLD response measurements, whereas low frequency oscillations represent task demands, not sensory inputs per se. In line with the interpretation that low frequency oscillations reflect pulsed inhibition, we speculate that suppression of low frequency oscillations amplifies neural activity in VTC in support of visual task demands.

Introduction

The task performed by an observer influences how the brain processes sensory inputs. Functional MRI (fMRI) studies have shown, in particular, that experimental tasks influence visually evoked activity in ventral temporal cortex (VTC; ***Huk and Heeger 2000***; ***Kay et al. 2015***; ***Kay and Yeatman 2017***; ***Grotheer et al. 2018***). One of these studies showed large increases in BOLD response amplitude during an image categorization task compared to a fixation task (***Kay and Yeatman, 2017***). Even basic visual tasks like image categorization can involve many aspects of cognition, such as perceptual decision making, memory retrieval, and semantic access (***Kay et al., 2023***). These cognitive task demands may have complex neural dynamics and understanding these dynamics requires

measurements with high temporal resolution.

The temporal dynamics of cognitive task demands on visual responses can be assessed using electrocorticography (ECoG). Measurements of ECoG high frequency broadband (HFB) activity (70-170 Hz) have been related to population input firing rates, and can measure neural responses with millisecond temporal resolution (***Miller et al., 2009a***; ***Manning et al., 2009***; ***Ray and Maunsell, 2011***; ***Hermes et al., 2017***). While fMRI measurements indicate that task demands change visual responses, temporally resolved measurements, like ECoG HFB, are necessary to reveal the temporal dynamics of cognitive task demands. Tasks might influence the overall state of the visual system and affect the way in which visual information arrives in V1 (***Luck et al., 1997***; ***Kastner et al., 1999***; ***Ress et al., 2000***; ***Giesbrecht et al., 2006***; ***Silver et al., 2007***; ***Buracas and Boynton, 2007***; ***Murray, 2008***). Or, tasks may highlight processing demands from higher order areas and affect the neural processing of visual responses at later times, i.e., 200 ms after the initial visual response (***Ogawa and Komatsu, 2004***; ***Halgren et al., 2006***; ***McDonald et al., 2010***; ***Davidesco et al., 2013***; ***Martin et al., 2019***).

Besides HFB, ECoG also allows the assessment of low frequency band (LFB) in the alpha/beta range (8-28Hz). LFB has been proposed to reflect pulsed inhibition (***Jensen and Mazaheri, 2010***; ***Schalk, 2015***). However, in the context of cognitive experiments, it is not well understood how sensory inputs and task demands influence alpha and beta oscillations. Visual alpha power is well known to peak during rest and decrease with visual input (***Berger, 1929***; ***Adrian and Matthews, 1934***), and has been modeled with visual encoding models (***Yuasa et al., 2023***). In contrast, other studies have shown that changes in attentional focus modulate alpha oscillations in visual areas (***Osaka, 1984***; ***Ray and Cole, 1985***; ***Jensen and Mazaheri, 2010***; ***Babu Henry Samuel et al., 2018***; ***Bonnefond and Jensen, 2024***). It is thus important to separate the contribution of visual inputs and task demands on alpha/beta power changes.

To better understand how cognitive tasks dynamically change neurophysiological processing in vision, we measured ECoG signals in two human subjects who had subdural electrodes implanted in early visual cortex (EVC) and ventral temporal cortex (VTC) for clinical purposes. We took advantage of a paradigm introduced in a previous fMRI study where subjects performed fixation and categorization tasks while they looked at words and faces of varying contrast (***Kay and Yeatman, 2017***). By holding stimuli constant and manipulating the task performed, the paradigm helps disentangle the contributions of stimulus processing and task demands to neural responses. Our results reveal how ECoG HFB and LFB dynamically capture visual input and cognitive task demands.

Results

In order to understand how task demands affect the neurophysiological processing of visual inputs, two patients with ECoG electrodes implanted for epilepsy monitoring performed, in separate runs, a fixation task and a categorization task while they looked at word, face and other stimuli (***Figure 1***). These stimuli varied in contrast and phase coherence. During the fixation task, subjects pressed a button when a central dot turned red, irrespective of the stimulus. This served as a control task to minimize the influence of task demands on how sensory information is processed. During the categorization task, subjects pressed a button to indicate whether the stimulus was a word, face, or neither, while still maintaining fixation on the central dot. Categorization required subjects to make a perceptual decision, which both subjects were able to do well (with 83-100% accuracy, ***Figure 1—figure Supplement 1***). Both subjects were faster at categorizing high contrast stimuli compared to lower contrast stimuli (average reaction times for highest and lowest contrast stimuli in Sub-1: 0.85 s ± 0.05 SEM and 1.00 s ± 0.07 and in Sub-2: 1.65 s ± 0.10 and 1.84 s ± 0.07). Consistent with many psychophysiological experiments (***Pins and Bonnet, 1996***; ***Barbur et al., 1998***; ***Plainis and Murray, 2000***), the longer reaction times during categorization of lower contrast stimuli suggests that task demands are higher for low contrast compared to high contrast stimulus conditions. While subjects were overall faster to categorize face stimuli with higher phase coherence compared to faces with lower phase coherence, the differences in reaction times between phase

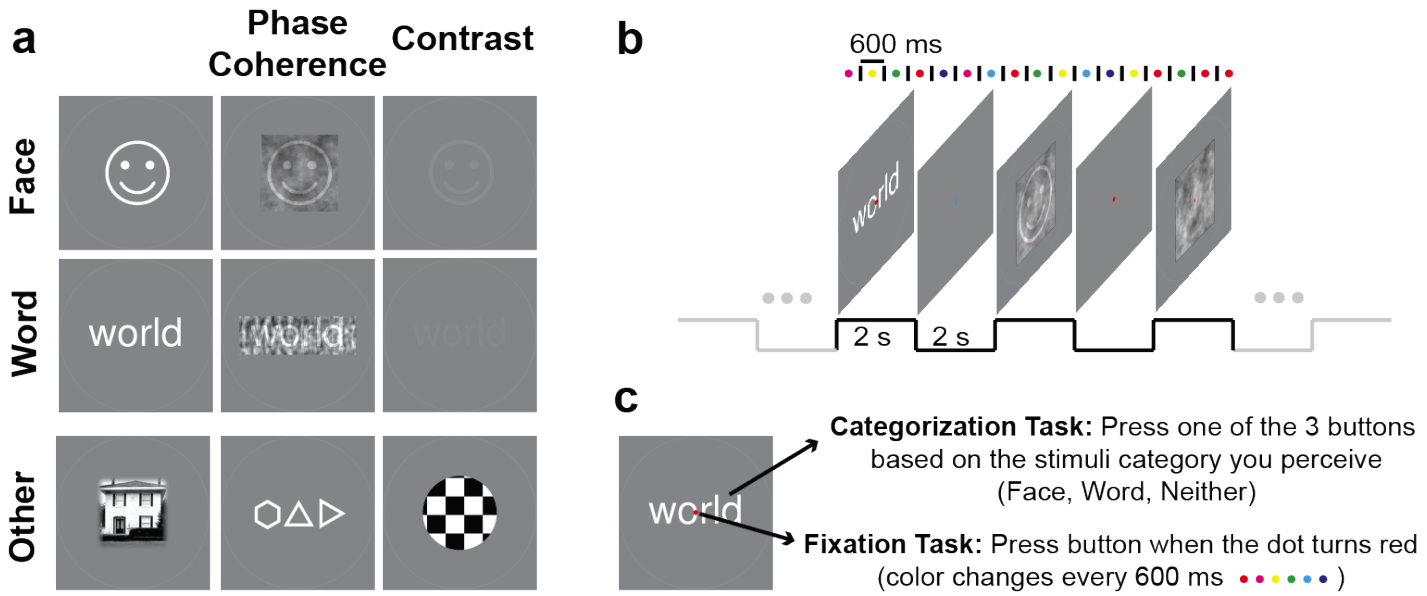

Figure 1. Experiment task design. (a) *Stimuli.* Stimuli included faces and words presented at different contrasts and phase-coherence levels, as well as full-contrast houses, polygons, and checkerboards. Faces shown here is for illustration purpose only. During the experiment pictures of human faces were shown (see Stimuli and Tasks for details.) (b) *Run.* Each run consisted of all the stimuli interleaved with a blank screen, with each stimulus presented thrice in a random order. Notice that the fixation dot changed color independent of the change of stimulus. (c) *Tasks.* On a given run, subjects performed either a fixation or a categorization task.

Figure 1—figure supplement 1. Behavioral response.

coherence variations for word stimuli were smaller (***Figure 1—figure Supplement 1***). To best capture how neurophysiological processes change with task demands, we therefore focus the ECoG results on the responses to contrast variations and show results for phase coherence in the supplement.

Visual stimuli and task demands induce independent HFB and LFB changes

Robust visual responses were measured in 19 electrodes across the two subjects ($n_{Sub-1} = 11$, $n_{Sub-2} = 8$). These electrodes were grouped into early visual cortex (EVC) and ventral temporal cortex (VTC) electrodes, located anterior and posterior to the posterior transverse collateral sulcus (ptCOS), respectively (***Figure 2a&b***). The visual stimuli induced HFB power increases as well as LFB power decreases. Spectrograms, in example EVC and VTC electrodes in each subject, show that HFB increases were highest during the first 0-1 s of stimulus presentation, and gradually reduced for the remainder of the stimulus duration of 2 s (***Figure 2c&d***). LFB power decreases were relatively smaller and most evident after ~0.2 s, after evoked response related power changes are resolved. These HFB and LFB changes are consistent with previous ECoG studies of visual cortex (***Hermes et al., 2015***; ***Jacques et al., 2016***).

In order to understand whether the HFB and LFB power changes capture different aspects of the same underlying neurophysiological signal or are independent signals, we performed a spectral principal component analysis (PCA). The spectral PCA naively extracts spectral features without preselection of a specific frequency range, and will result in separate components if stimuli and task conditions have different effects on low and high frequencies (for details, see ***Miller et al. 2009a***). The spectral PCA identified a broadband component as the first principal spectral component (PSC) and a low frequency component as the second PSC (***Figure 2—figure Supplement 1c&d***). The low frequency component ranges from ~8-28 Hz and captures alpha and beta oscillations, indicating that in our experiment these low frequencies (8-28 Hz) fluctuate together. These two PSCs in broadband and low frequency range are consistent with previous studies (***Miller et al., 2009a***;

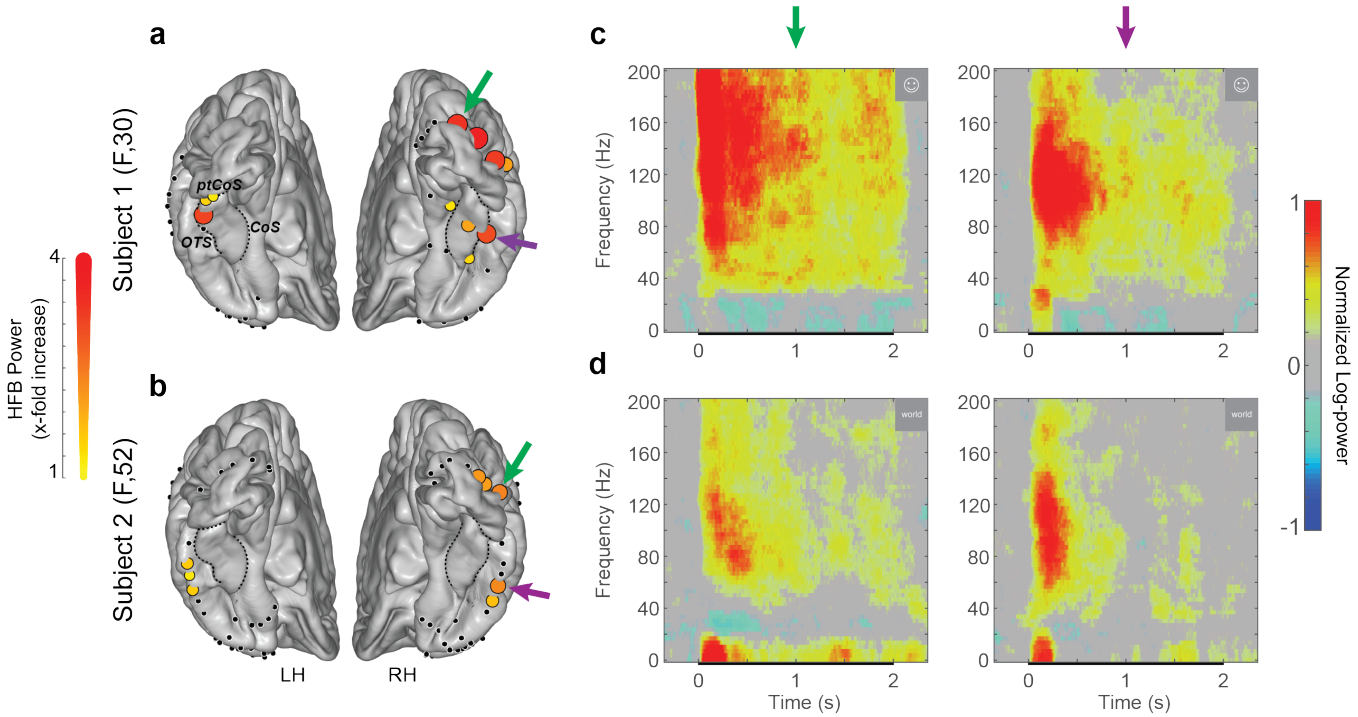

Figure 2. Electrode locations and spectral power changes. (a,b) ECoG electrode locations in subject 1 (top) and subject 2 (bottom). Visual-responsive electrodes are shown in colored circles; color and size of the circle indicates the intensity of time-averaged HFB power (0-400 ms, face & word responses at 100% contrast). (c,d) Time-frequency power (spectograms) for an EVC electrode (green arrow) and a VTC electrode (purple arrow) in each subject. The inset shows the stimulus (face/word at 100% contrast) for which the plots were computed. Black bars on the time axis indicate duration during which stimulus was presented (0-2 s). *COS*: collateral sulcus, *ptCOS*: posterior transverse COS, *OTS*: occipital-temporal sulcus

Figure 2—figure supplement 1. Power spectral components

Sabra et al., 2020) and reveal that these two components change independently across stimulus and task variations. Moreover, this indicates that HFB and LFB power changes likely represent different neurophysiological processes. These observations from our data-driven PCA analysis justify our choices of how to quantify HFB and LFB power changes: we compute HFB increases by filtering ECoG responses in 70-170 Hz and LFB suppression by filtering responses across the alpha/beta range in 8-28 Hz (***Figure 4***,***Figure 5***,***Figure 6***). Supplementary analyses of power changes based on the spectral PCA components and separate alpha and beta bands show similar results (***Figure 5—figure Supplement 2***, ***Figure 6—figure Supplement 2***).

Task demands transiently increase HFB responses in a stimulus specific manner

HFB responses can reveal the timing of the effects of task demands on neural activity. As described in the previous fMRI study, BOLD responses were shown to scale with task demands (***Kay and Yeatman, 2017***). To test whether this scaling affects the entire response duration or has a transient effect (represented in schematics in ***Figure 3***), we calculated time-varying HFB responses. We show that the HFB responses encoded stimulus features and were affected by the task as follows.

First, HFB responses encoded stimulus features in a way that replicates previous ECoG studies (e.g. ***Groen et al. 2022***). Increasing stimulus contrast resulted in larger HFB responses throughout EVC, FFA and vWFA, regardless of the task (***Figure 4***). Moreover, the time-to-onset and the time-to-peak both decreased with increasing stimulus contrast (time-to-onset: $\beta = -147.36,\ S.E. = 19.43, p < 10^{-5}$, time-to-peak: $\beta = -141.11,\ S.E. = 23.28, p < 10^{-5}$; ***Figure 4—figure Supplement 1&5***). The temporal dynamics of the HFB response further show that high contrast words and faces induced large initial responses for 1 s following the stimulus onset, which was then followed by a

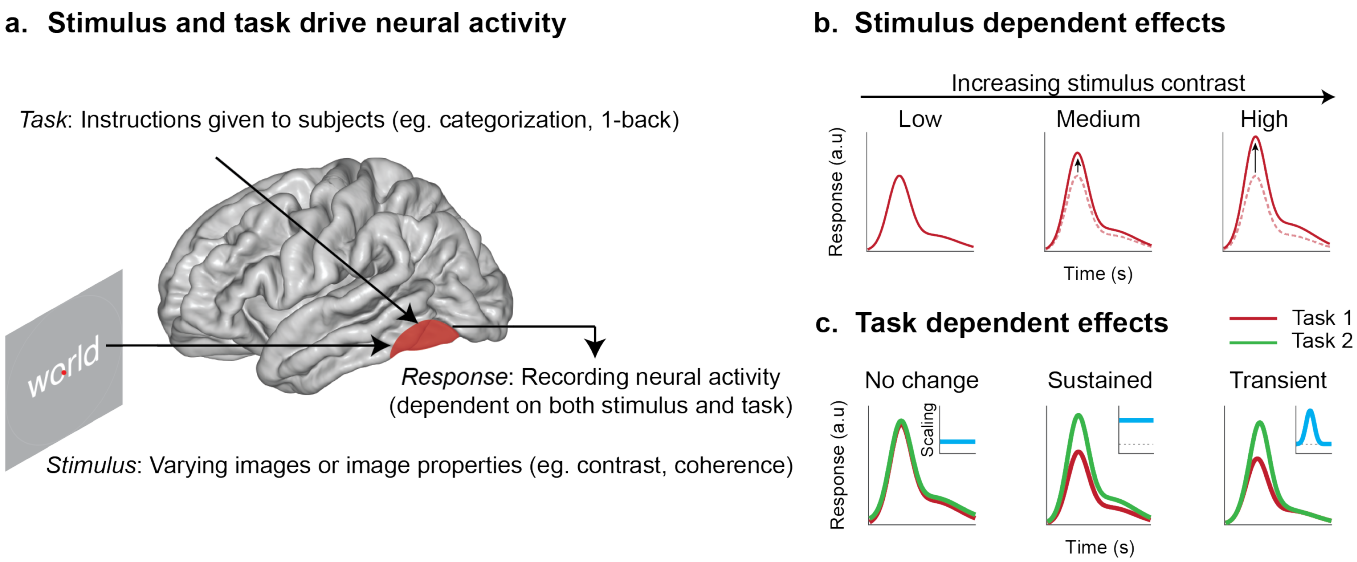

Figure 3. Schematics of stimulus and task driven visual responses. (a) Schematically showing that recorded neural activity is dependent on both stimulus and task. (b) Schematics of stimulus dependent increases in ECoG HFB responses at three increasing levels of contrast. The dotted trace indicates the response at low contrast. (c) Schematics showing task effects when there is no differences in the responses across two tasks (left), sustained effects with constant scaling (middle), and transient scaling (right). Cyan traces in the insets indicate scaling factor (ratio of responses of Task 2 over Task 1). The dashed line indicates no scaling.

smaller sustained response until 2 s, after which the HFB power returned to the baseline. These delays and onset transients are consistent with previous modeling and empirical studies (***Zhou et al., 2018***, ***2019***).

Second, the HFB responses were affected by the task performed by the subject. During categorization, HFB responses were typically larger compared to fixation. For example, responses to word stimuli at 5% contrast during fixation peaked at less than 1-fold HFB increase compared to baseline, whereas during categorization, responses increased by more than 2-fold. These increases were particularly pronounced for lower contrast stimuli, and may be indicative of increased task demands required to categorize these lower contrast stimuli (***Kay and Yeatman, 2017***).

To quantify the temporal profile of this task-related scaling, we calculated time-resolved scaling factors as the ratio of the HFB response during categorization over fixation (***Figure 4*** insets, cyan traces indicate significant scaling ($p < 0.05$, cluster-based permutation test)). Task-related scaling effects were transient; the scaling factor had an onset around 0.2 s (range: $0.190 - 0.600s$, mean: $0.360s + / - 0.040SEM$ and typically lasted for <1 s (with one exception in ***Figure 4c***, left panel). These scaling effects were observed for faces and words in the EVC (***Figure 4a&c***). Word selective electrodes in the VTC (visual word form area, vWFA) showed strong, transient scaling for low contrast word stimuli (***Figure 4b***). Similarly, face selective electrodes in the VTC (fusiform face area, FFA) showed strong, transient scaling for low contrast face stimuli (***Figure 4d***). Scaling was also present in non-selective VTC electrodes as well as for non-preferred stimuli in vWFA and FFA, but the overall response magnitudes were smaller (***Figure 4—figure Supplement 3&4***). While the previous fMRI study showed that BOLD responses were increased during categorization, our results further reveal that increases in neural activity are not present during the entire response period, but are visible most strongly during ~0.2-1 s. Thus, ECoG provides us with temporal information of these task-related increases, i.e., task demands are more reflected in the transient period with a delayed onset and are not sustained for the entire response period.

ECoG HFB responses match fMRI BOLD

Previous studies that compared BOLD and field potential measurements reported a strong correlation between the fMRI BOLD response and the ECoG HFB changes (***Hermes et al., 2015***, ***2017***;

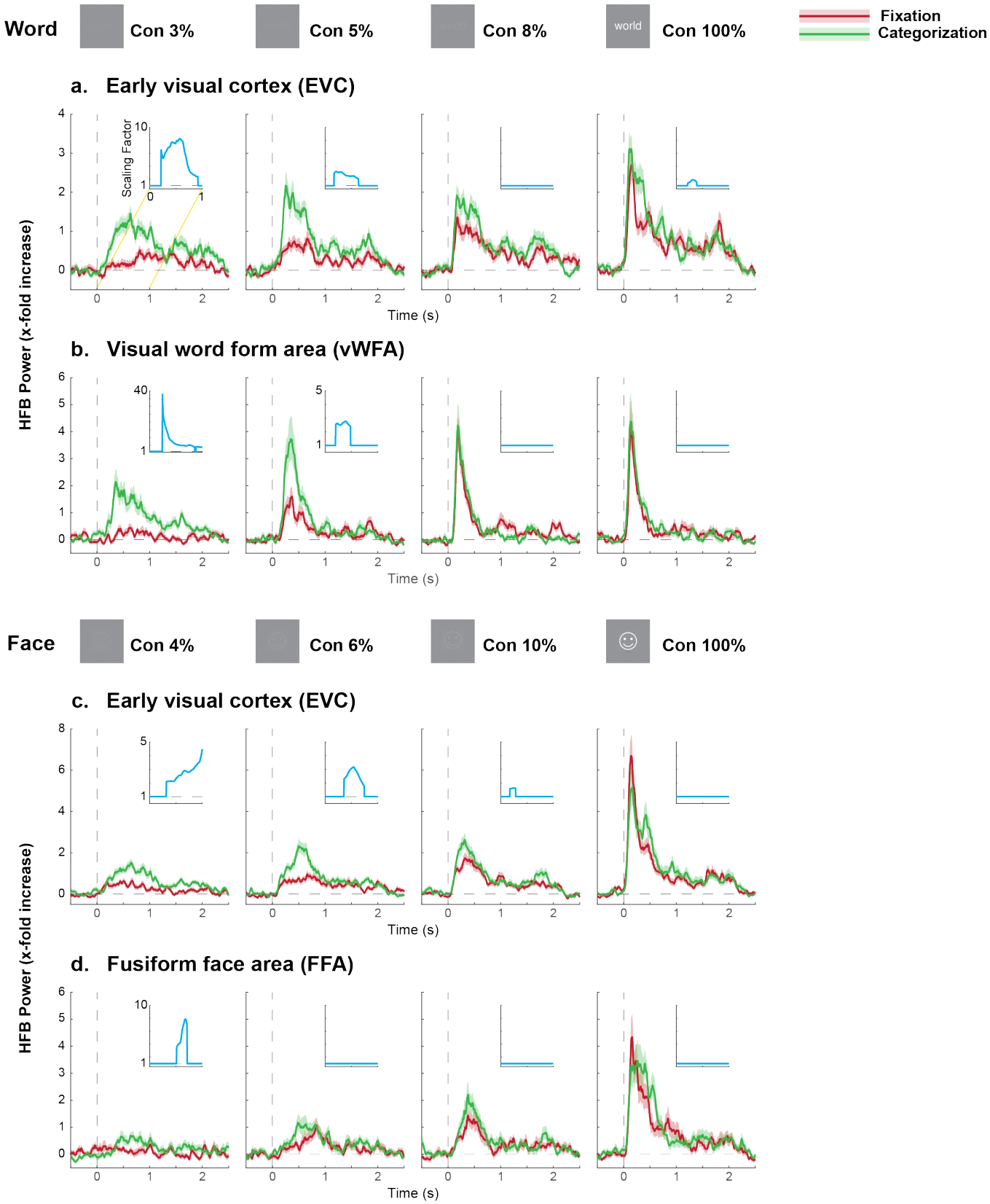

Figure 4. Stimulus and task effects in ECoG HFB. ECoG HFB power traces during fixation (red) and categorization (green) with increasing stimulus contrast (word/face, shown on the top). The average HFB power (solid) was calculated by geometric averaging over electrodes and trials. The shaded region corresponds to the 68% confidence interval. The horizontal dashed lines indicate baseline and the vertical dashed lines indicate the stimulus onset. The inset in each plot corresponds to the scaling factor calculated as the ratio of HFB power of the categorization over the fixation task. (*contd. on the next page*)

Figure 4. (*Previous page*.) Cyan traces deviated from 1 (grey dashed line) when scaling effects were significant (p<0.05; cluster-based permutation test). Dashed line at 1 indicate no scaling (a,b) HFB power for increasing word contrast in EVC and vWFA. (c,d) HFB power for increasing face contrast in EVC and FFA.

Figure 4—figure supplement 1. Temporal characteristics of HFB power increases.

Figure 4—figure supplement 2. HFB power increases during phase coherence variation.

Figure 4—figure supplement 3. HFB power increases during contrast variation (non-selective electrodes).

Figure 4—figure supplement 4. HFB power increases during phase coherence variation (non-selective electrodes).

Figure 4—figure supplement 5. Summary plots of HFB power increases across stimulus manipulation.

Jacques et al., 2016). Our results are consistent with these findings. The previous fMRI study (***Kay and Yeatman, 2017***) showed that BOLD responses were increased during categorization compared to fixation, and this increase was the strongest during low contrast conditions with high task demands (***Figure 5a***). We compared these BOLD signal changes from the previous study to the time-averaged HFB responses from 0-1 s (***Figure 5b***). Time-averaged scaling factors were calculated as the ratio of the averaged HFB responses during categorization over fixation. The modulatory scaling effects are remarkably similar across the two measurement modalities, with lower contrast conditions showing large increases in task-related scaling. Therefore, both modalities indicate that increased response scaling is observed with higher cognitive task demands.

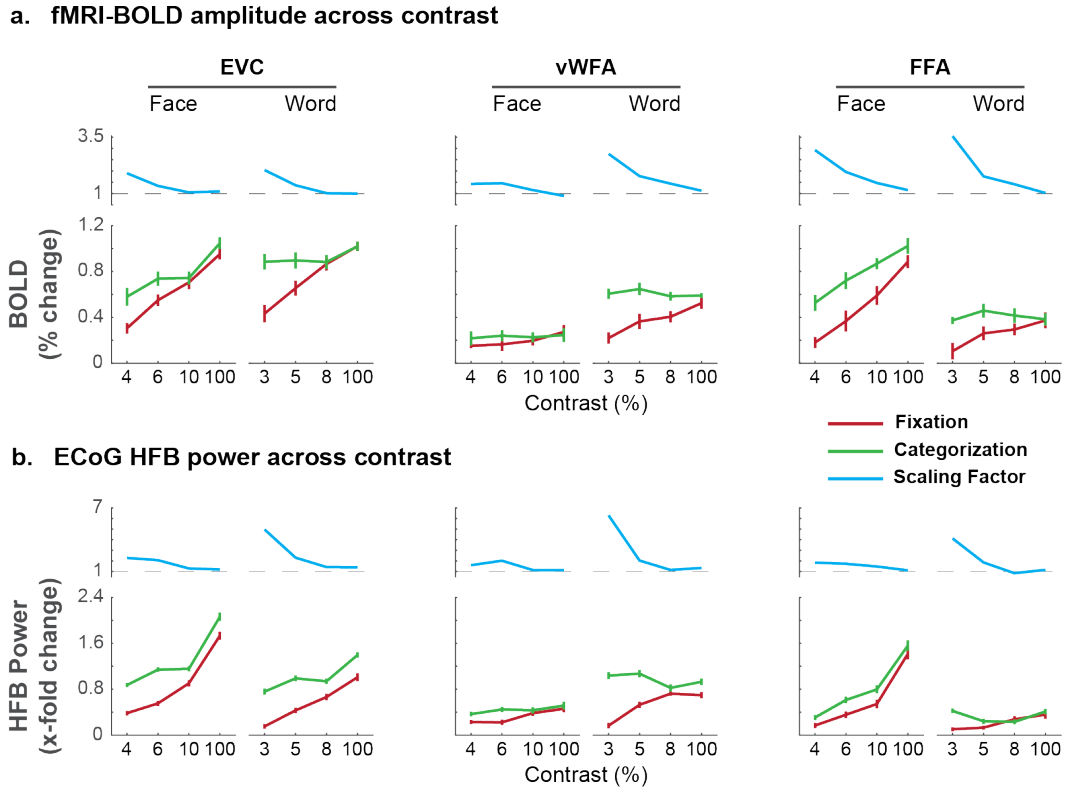

Figure 5. Time-averaged ECoG HFB responses match fMRI BOLD amplitudes. (a) fMRI BOLD responses reproduced from (***Kay and Yeatman, 2017***) for varying stimulus contrast for EVC (left) vWFA (middle) and FFA (right). (b) ECoG HFB responses time-averaged in 0-1 s time window. Cyan traces show scaling factors with horizontal dashed line at 1 indicating no scaling. Verticals bars indicate 68% confidence interval.

Figure 5—figure supplement 1. Time-averaged ECoG HFB responses match fMRI BOLD amplitudes for phase coherence manipulations.

Figure 5—figure supplement 2. PSC-based HFB responses for contrast and phase coherence manipulations.

Low frequency alpha/beta power decreases depend on cognitive task demands

Decreases in alpha/beta power observed during visual processing could in theory reflect either the encoding of stimulus properties or the demands of the task. A critical aspect of our experiment is that we measured responses to the same stimuli under multiple tasks, making it possible to disentangle stimulus properties from task demands. To investigate alpha/beta power, we calculated LFB power changes from 8-28 Hz, and this was done over the time window 0.25-1.25 s to minimize contamination from the evoked response. LFB power decreased after the initial evoked response during both tasks, with larger suppression observed during categorizaiton (***Figure 6a***). Moreover, the magnitude of the LFB power changes was different for the two tasks. During the fixation task, LFB power decreased in a comparable magnitude from baseline across low and high contrast conditions (***Figure 6b***, red lines). However, during the categorization task, LFB power suppression varied across stimulus contrast, with ~3-fold larger decreases during the lowest contrast stimulus compared to the highest contrast stimulus (***Figure 6b***, green lines). The stronger LFB decreases when categorizing low contrast face and word stimuli was consistently observed across EVC, FFA and vWFA.

In order to formally test whether the stimulus contrast affected LFB power, we averaged LFB power across stimulus types and fit a first order polynomial relating contrast to the response (***Figure 6c*** dotted lines). On the one hand, the line fit for the fixation task does not have a slope that is significantly different from 0 ($\beta = 0.01,\ p = 0.34$), which suggests that the LFB suppressions during the fixation task do not encode the stimulus variations. Instead, the constant amount of LFB

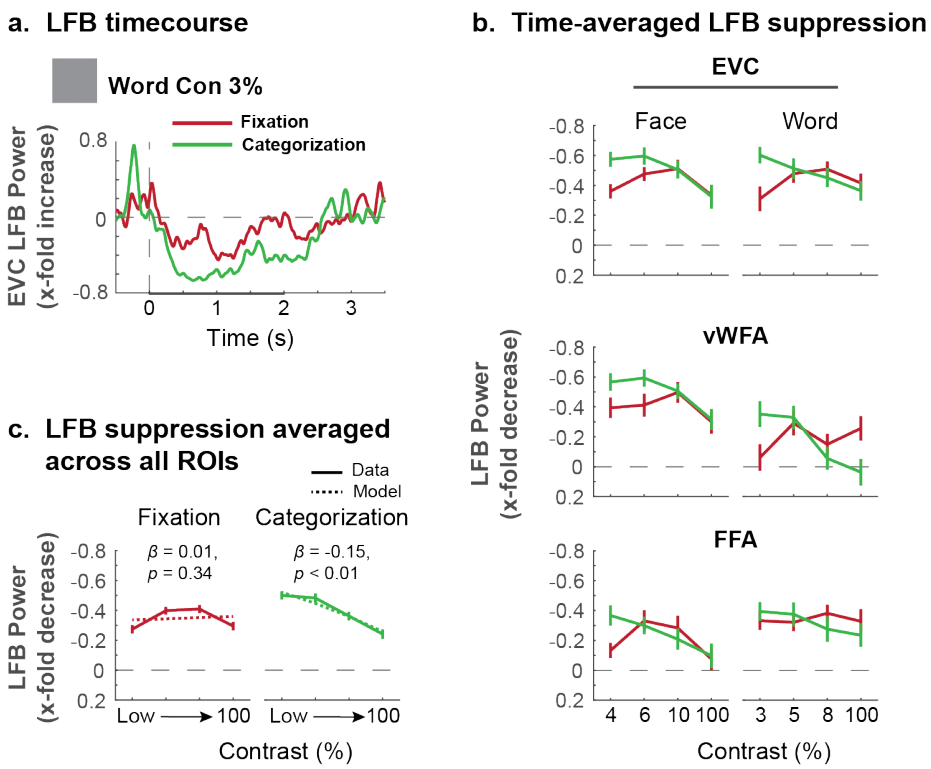

Figure 6. Time-averaged ECoG LFB responses reflect task demands. (a) LFB power time course shown for 3% word contrast averaged across all EVC electrodes, as an example. Thick black bar 0-2s on x-axis indicates the duration of stimulus presentation (b) LFB power suppression time-averaged in 0.25-1.25 s time window. (c) LFB suppression for faces and words combined and averaged across all the EVC, vWFA, and FFA electrodes. Dotted line indicates the best linear fit with slope β. Vertical bars indicate 68% confidence interval. Note: the vertical axis in b & c is inverted to emphasize LFB suppression.

Figure 6—figure supplement 1. Temporal characteristics of LFB power suppression.

Figure 6—figure supplement 2. Time-averaged ECoG LFB suppression across different conditions.

suppression may suggest an automatic LFB suppression induced by a general engagement of the visual system. On the other hand, the line fit for the categorization task shows a significant negative slope ($\beta = -0.15,\ p < 0.01$), which indicates that the LFB suppression during categorization decreases with higher stimulus contrast. Whereas task demands are relatively constant during the fixation task (where the subject continuously monitors the color of the fixation dot), the categorization task is most difficult in low contrast conditions and easiest during high contrast conditions. During the categorization task, LFB suppression therefore appears to reflect task demands. Overall, this pattern of LFB decreases suggests that visual input induces a constant LFB suppression and additional variations in the amount of LFB suppression reflect task demands.

Discussion

Experimental task demands influence how visual inputs are processed by the brain. We measured ECoG signals in human visual areas to characterize neural processing of visual inputs during two different tasks. We found two independent neurophysiological signals, one that captured broadband high frequency power and one that captured low frequency alpha/beta oscillations, that encoded visual inputs and task demands. As expected, HFB responses encoded stimulus contrast, and increased with higher contrast. HFB responses additionally exhibited modulation by task demands in terms of task-related scaling effects, which especially increased HFB responses during difficult categorization conditions. Extending beyond what was previously shown in fMRI BOLD, we found that task-related scaling in local neuronal activity is transient, starting 0.2 s post stimulus onset and typically lasting < 1 s. Surprisingly, LFB responses were not driven by stimulus contrast and therefore do not seem to encode stimulus properties per se. Rather, LFB responses appear to reflect task demands, showing stronger suppression for more difficult categorization conditions.

Low frequency power suppression encodes task demands

In the fixation task, LFB power suppression was relatively comparable across different stimulus conditions. In the categorization task, LFB power suppression was stronger when the task was more difficult. This indicates that while LFB power may be sensitive to general visual input, LFP power does not primarily encode image properties like contrast. A general sensitivity to visual input was found in a previous study showing that alpha suppression was spatially tuned to visual inputs with relatively large receptive fields (***Yuasa et al., 2023***). Alpha power may thus be sensitive to stimuli in the population receptive field. However, the level of alpha decreases may be driven by task demands rather than the image content in the receptive field per se. This interpretation is consistent with laminar recordings in macaque V1 that showed that alpha power decreased when an unattended visual stimulus was presented compared to when an auditory stimulus was presented, but decreased much more when subjects paid attention to the visual stimulus (***Bollimunta et al., 2011***). These results are also consistent with previously reported alpha suppression related to attentional demands (***Osaka, 1984***; ***Ray and Cole, 1985***; ***Jensen and Mazaheri, 2010***; ***Babu Henry Samuel et al., 2018***). There are thus likely two processes that guide low frequency power changes in visual areas. One is generically induced by visual input and suppresses overall low frequency power and a second that is driven by task demands and regulates the specific magnitude of the decrease.

Large low frequency alpha and beta oscillations at rest have been proposed to reflect pulsed inhibition of local neuronal firing (***Jensen and Mazaheri, 2010***; ***Miller et al., 2012***; ***Schalk, 2015***). In this framework, pulsed inhibitory inputs suppress the membrane potential to inhibit local neuronal firing. Decreases in LFB power release the inhibition over task-relevant regions. The larger decreases in LFB power during difficult stimulus categorization conditions may be reflective of a release of inhibition that facilitates local neuronal computation—for example, the upregulation of sensory-related signals in VTC may help inform decision-related processes performed in the intraparietal sulcus (***Kay and Yeatman, 2017***). EEG studies have indeed linked low frequency power suppression to a state of optimal excitability in the underlying neuronal population (***Rajagovindan***

and Ding, 2011). High alpha power, conversely, may inhibit neuronal computation and serve as a gate for feedforward flow (*Zhigalov and Jensen, 2020*). Overall, we suggest that changes in alpha and beta power may facilitate the contribution of local neuronal processing to the performance of different visual tasks.

High frequency broadband response scaling is transient

The ECoG recordings enabled us to estimate the time window during which task demands scale neural responses. The HFB response increases during difficult categorization conditions compared to fixation were observed transiently from ~0.2-1 s post stimulus onset. The scaling effects thus do not start with response onset nor do they last for the duration of the stimulus. These transient scaling effects are in line with the brief control signals postulated to shift cognitive states rather than a continuous signal actively maintaining the modulated state (*Yantis et al., 2002*). Indeed, the hypothesis of brief control signals is consistent with our prior observation (*Kay and Yeatman, 2017*) that the amount of scaling is specific to the stimulus, in a way that appears to be related to the task being performed by the subject (e.g. evidence accumulation for perceptual decision making).

The fact that the scaling is observed relatively late supports the idea that the scaling is the result of feedback inputs to VTC. Feedback inputs to visual areas during the categorization task were previously modeled as inputs from the intraparietal sulcus (*Kay and Yeatman, 2017*). Moreover, this study measured fMRI BOLD changes in parietal areas during the same tasks and found that parietal responses predicted the gain measured in the VTC. While the frontal eye fields (*Gilbert and Li, 2013*) and subcortical structures like the pulvinar (*Desimone et al., 1995*; *Saalmann et al., 2012*) likely also play a role in task modulation, inputs from parietal cortex are a strong candidate for potentially driving the measured task modulations of visual cortex. Firstly, anatomical tracing and human diffusion MRI studies have indeed shown that parietal cortex and visual ventral temporal areas are directly connected (*Felleman and Van Essen, 1991*; *Distler et al., 1993*; *Webster et al., 1994*; *Markov et al., 2014*; *Yeatman et al., 2014*; *Takemura et al., 2016*; *Bullock et al., 2019*; *Panesar et al., 2019*; *Vinci-Booher et al., 2022*). Secondly, TMS studies have further shown that parietal stimulation can change the excitability in early visual areas V1/V2 (*Silvanto et al., 2009*; *Capotosto et al., 2009*, *2012*). While our subjects did not have electrodes placed on parietal areas, such measurements could provide information on the neurophysiological basis of dorsal and ventral interactions during different visual tasks.

Task-related scaling is consistent with flexible modulation

The measured HFB responses increased with stimulus contrast and this contrast response function was modulated during the categorization task. Specifically, categorization increased HFB responses for low contrast conditions. These contrast response functions can shift in different ways with cognitive processing, and previous studies proposed four models that capture different types of shifts observed across various visual paradigms (*Zhang and Kay, 2020*). First, an additive-shift model predicts an increase in neural activity of comparable magnitude across all contrast conditions (*Luck et al., 1997*; *Kastner et al., 1999*; *Ress et al., 2000*; *Giesbrecht et al., 2006*; *Silver et al., 2007*; *Buracas and Boynton, 2007*; *Murray, 2008*). Second, a response-gain model multiplies the responses by a gain factor, which results in increased gain for high amplitude responses to high contrast stimuli (*McAdams and Maunsell, 1999*). Third, a contrast-gain model predicts increased sensitivity by horizontally shifting the contrast response function and results in the largest response increases for mid-contrast stimuli (*Reynolds et al., 2000*). Lastly, a flexible modulation model predicts that the experimental task scales responses in relevant regions in order to process specific stimuli and meet certain task demands (*Zhang and Kay, 2020*). The flexible modulation model best explains the data from the previous fMRI study as well as our current measured ECoG HFB responses. The increased reaction times during low contrast conditions are consistent with the interpretation that task demands were higher during these conditions, and the flexible modulation model accordingly posits that neural responses are higher during these conditions.

Significance of task sampling for interpreting neural responses

Our findings demonstrate the importance of considering the task when evaluating and interpreting the relation between visual inputs and neural responses. If we had sampled neural responses only while subjects performed the fixation task, we would have observed a constant LFB suppression irrespective of the stimulus presented. This may have led to the incorrect interpretation that LFB suppression was irrelevant to visual processing. On the other hand, if we had sampled neural responses only while subjects performed the categorization task, we might have come to the incorrect interpretation that LFB encodes stimulus contrast. Only through a more comprehensive sampling of stimuli and tasks were we able to reach our current interpretation that LFB decreases encodes task demands, rather than stimulus properties per se. Of course, it will be important in future work to sample an even larger range of tasks and stimulus types in order to strengthen support for our current interpretation of low frequency alpha and beta oscillations.

Methods and Materials

Subjects

The experimental protocol was approved by the Institutional Review Board of Baylor College of Medicine. Two patients (F/30 (Sub-1) and F/52 (Sub-2)) with medically refractory epilepsy, who had intracranial electrode arrays (AdTech) implanted for clinical epilepsy monitoring to localize seizure foci before surgical treatment, consented to participate in the study. A third patient also consented, but had a lesion near the vWFA and had difficulty seeing the stimuli and so was excluded from the study.

Electrode locations were estimated based on the operative sketch, and are displayed on the MNI (Montreal Neurological Institute)-152 template brain to provide a schematic overview (***Figure 2a&b***). These are not meant to perfectly capture the anatomy, and we note that none of the analyses performed in this paper depend on detailed anatomical labeling. We grouped electrodes into those reflecting early visual areas (EVC, posterior to the posterior transverse collateral sulcus (ptCOS)) and those reflecting ventral temporal cortex (VTC, anterior to ptCOS).

Stimuli and Tasks

Subjects were presented with face and word stimuli, varying in contrast and phase coherence, with a central fixation dot that changed color every 600 ms. The stimuli and tasks were the same as used in the previous fMRI study (***Kay and Yeatman, 2017***). The face stimuli (faces101:7) were made freely available without copyright restriction from the lab of Dr. Kalanit Grill-Spector. Face stimuli were presented at 4%, 6%, 10%, and 100% contrast levels whereas word stimuli were presented at 3%, 5%, 8%, and 100% contrast levels. Both sets of stimuli were also presented at 0%, 25%, 50%, 75%, and 100% phase coherence levels. Other control stimuli consisting of houses, checkerboards, and polygons were also presented but not considered in our analyses.

In separate runs, the subjects were asked to perform a fixation task and a categorization task. The fixation task is intended to minimize the influence of task demands on how the stimuli are processed. The categorization task is intended to probe how task demands influence sensory processing.

Fixation task: The subjects were asked to press a button whenever the fixation dot turned red. The dot changed color every 600 ms in a random order to one of six colors: magenta, red, yellow, green, cyan, and blue. Dot color changes were continuous (i.e., no rest) and the timing of the dot changes (every 600 ms) was independent of the presentations of the stimuli (every 2 s). This was intentional to minimize any potential interactions between the performance of the fixation task and responses to the stimuli.

Categorization task: The subjects were asked to press one of three buttons – word, face, or neither – based on the stimulus category they perceived. Subjects were instructed to respond

within 4 s of stimulus onset (this coincided with 2 s of stimulus presentation plus 2 s of rest/blank presentation).

The task was adjusted for the ECoG setting, and therefore differed slightly from the miniblock design used previously during fMRI (***Kay and Yeatman, 2017***) . During ECoG, each run consisted of 68 trials: 1 blank trial, 66 stimulus trials, and 1 blank trial. During each stimulus trial, the stimulus was presented for 2 s followed by rest (blank) for 2 s. Both subjects performed 2 runs of each task in the order of FCFC (F: fixation, C: categorization). Each stimulus (e.g., face at 3% contrast) was presented three times during each run giving a total of 6 trials for each combination of stimulus and task for each subject. The viewing distance for the experiment was approximately 60 cm, and the stimuli were approximately 2° tall and wide (see ***Figure 1***). A faint circle (10% opacity, 4.2° diameter) surrounding each stimulus was shown for subject 1 to help them realize when the stimuli were present, and this circle was presented identically for all stimuli. Unlike the previous fMRI study, we did not conduct a one-back task in the ECoG study.

ECoG recording

ECoG data were recorded at 2000 Hz from a Blackrock neural signal processor. Non-recording electrodes (as well as electrodes near the seizure onset zone) were identified based on clinical notes and were excluded from analysis. Raw signal from the remaining electrodes was first filtered (5th order Butterworth IIR notch) for line noise removal at 60 Hz and its harmonics. Common average re-referencing (CAR) was then performed to remove other electrical noise common to all electrodes. Data were reviewed and epochs with artifacts (sharp transients and interictal discharges) were removed.

ECoG time varying HFB and LFB responses

The signal from each electrode was bandpass filtered (2nd order Butterworth IIR), in frequency bins of 5 Hz; 70-170 Hz for high frequency broadband (HFB) and 8-28 Hz for lower frequency (LFB; alpha/beta) oscillations. Then, the absolute value of the Hilbert transform was calculated and the geometric mean was taken across bands (to ensure that lower and higher frequency bands contributed relatively equally to the average). Next, the power of the signal was calculated and the signal was downsampled to 200 Hz. We calculated the x-fold signal change with respect to the prestimulus baseline power (e.g. power of 2 during baseline and power of 8 during stimulus is a 3-fold increase: $\frac{8}{2} - 1$), resulting in a percent signal change for each electrode. The prestimulus baseline was defined as 500 ms to 100 ms before stimulus onset, and baseline power was averaged across time and conditions using the geometric mean. The HFB or LFB percent signal changes are plotted with respect to 0 (no change) as power increases or decreases.

Visually responsive electrodes were identified as electrodes with significant HFB power increases ($p < 0.01$ by right-tailed sign test, Bonferroni corrected for multiple comparisons across all electrodes) in the 0-400 ms time window post stimulus onset, pooling across all full contrast conditions. These visually responsive electrodes were classified based on anatomical location as reflecting early visual cortex (EVC; $n_{Sub-1} = 4,\ n_{Sub-2} = 3$) and ventral temporal cortex (VTC; $n_{Sub-1} = 7,\ n_{Sub-2} = 5$). Electrodes that were visually responsive, but not within these regions were not considered for our analysis ($n_{Sub-1} = 8,\ n_{Sub-2} = 3$). Similar as in other studies (***Jacques et al., 2016***), VTC electrodes were further classified into fusiform face area (FFA) and visual word-form area (vWFA) electrodes based on their d', calculated as

$$d' = \frac{\mu_w - \mu_f}{\sqrt{\frac{\sigma_w + \sigma_f}{2}}}$$

where μ_x is the average HFB response in 0-400 ms post stimulus onset, σ_x is the variance across 100% contrast trials, and $x \in \{w = word, f = face\}$. If $d' >= 1$, then electrodes were marked as vWFA ($n_{Sub-1} = 2,\ n_{Sub-2} = 3$), whereas if $d' <= 1$, then electrodes were marked as FFA ($n_{Sub-1} = 4,\ n_{Sub-2} = 0$). Other electrodes ($-1 < d' < 1$) were considered to be non-selective VTC ($n_{Sub-1} = 1,\ n_{Sub-2} = 2$) electrodes.

ECoG HFB scaling factor

To quantify the effect of cognitive task demands, a scaling factor was computed as the ratio of HFB power changes observed during the categorization task over HFB power changes observed during the fixation task. First, HFB responses (averaged across trials) were smoothed using a 200 ms moving average window. Then, the scaling factor was computed as the ratio of HFB response during the categorization task over HFB response during the fixation task for each condition. HFB responses that fell below baseline were set to 0.01 to avoid division by zero or negative numbers. We used cluster-based permutation testing that corrects for multiple comparisons (***Maris and Oostenveld, 2007***) to determine time points that were significantly ($p < 0.05$ different across the two tasks. Non-significant scaling factors were set to 1 (indicating no scaling).

Average HFB and LFB power changes

In order to compare the power changes observed in this study with the BOLD percent signal changes reported in (***Kay and Yeatman, 2017***), we time-averaged ECoG responses in a 1 second window post stimulus onset. HFB responses were averaged across a 0-1 s window to capture the bulk of the responses. LFB responses were averaged across a 0.25-1.25 s window that incorporated a slight temporal offset in order to minimize the effect of evoked responses.

Spectral visualization

To visualize spectrograms, we used a multi-taper time-frequency spectrum analysis (***Bokil et al. 2010***; 300 ms moving average window, 10 ms step size). Spectrograms for each condition were created by computing the median spectral response across trials. Baseline was calculated as the median across time (baseline window: 500 ms to 100 ms before stimulus onset) and conditions. Finally, spectrograms were log-normalized by computing the log and subtracting the baseline.

Principal spectral component analysis

Several studies have emphasized the importance of separating low frequency oscillations from the background $\frac{1}{f^n}$ power (***Miller et al., 2009b***; ***Hermes et al., 2019***). When filtering for low frequency bands, the overall power may be affected by a combination of spectral broadband change plus additional oscillatory signals. As a control analysis, we computed the power spectral components (PSCs; ***Miller et al. 2009a***) using principal component analysis (PCA). This data driven approach extracts components that explain the most variance across the power spectrum. In ECoG data, the first component often reflects broadband power and the second component often captures changes in lower frequencies (***Miller et al., 2014***). The PCA ensures that these features are orthogonal and changes in one are uncorrelated with changes in the other. First, the power spectral density was computed in four bins of 500 ms corresponding to data from 500 ms prestimulus to 1500 ms post stimulus onset. Next, the power spectrum was flattened (across tasks, stimuli, and trials) and was then log-normalized by taking log of the power spectrum and subtracting the average power spectrum. PCA on the power spectrum produced PSCs in decreasing order of variance explained. The first two PSCs were then considered for further analysis to ensure that low and high frequency band changes capture different processes, rather than different spectral features of the same process (***Donoghue et al., 2022***).

Time-to-onset, time-to-peak, and duration

To calculate temporal response features, responses were pooled across face and word conditions for EVC electrodes. For selective VTC electrodes, responses to faces from FFA electrodes and responses to words from vWFA electrodes were pooled. Next, we used cluster-based permutation testing that corrects for multiple comparisons (***Maris and Oostenveld, 2007***) to find time windows (within 0-1 s of ECoG response post stimulus) for which responses were significantly ($p < 0.05$) different compared to the prestimulus baseline for each task. Time-to-onset was then calculated as the initial time point of the first significant cluster and duration was calculated as the total length of

all the significant time windows (i.e., significant clusters). Lastly, time-to-peak was calculated as the time at which the response was maximum for each condition, again, within 0-1 s of ECoG response post stimulus. Statistical analysis was performed by fitting a linear mixed-effects model that predicted time-to-onset, time-to-peak, and duration, independently, with fixed effects for stimulus contrast x task x ROI (EVC/VTC), and an intercept-only random effect for subjects.

Behavioral response

Reaction time and accuracy were computed to evaluate subject's performance during the experiments. For both the tasks, reaction time was calculated as the time taken by the subjects for their first button press from stimulus onset. For the categorization task, in case of multiple responses only the first response was considered. If no response was recorded within 4 s after stimulus onset, the trial was considered as invalid and excluded from the behavioral analysis. Only one condition, face contrast at 4%, had two invalid trials in Sub-1. All other conditions had at least one response from both subjects. Average reaction times were then calculated as the median reaction time across all valid trials. Next, response accuracy for the categorization task was calculated as the percentage of correct responses across all valid trials. For the 0% and 25% phase coherence conditions, we considered the 'neither' response as correct.

Acknowledgments

The authors thank the patients and staff at the Baylor College of Medicine. We thank Kai Miller for his constructive feedback. Research reported in this publication was supported by the National Eye Institute of the National Institutes of Health under award numbers R01EY035533 (KK and DH), R01NS065395 (MSB) and R01EY023336 (DY). The content is solely the responsibility of the authors and does not necessarily represent the official views of the National Institutes of Health.

Additional information

Author contributions

Zeeshan Qadir: Software, Formal Analysis, Validation, Visualization, Writing-original draft, Writing-review & editing;
Harvey Huang: Software, Writing-review & editing;
Müge Özker: Investigation, Data Curation;
Daniel Yoshor: Investigation, Resources, Funding Acquisition, Writing-review & editing;
Michael S. Beauchamp: Methodology, Investigation, Resources, Funding Acquisition, Writing-review & editing;
Kendrick Kay: Conceptualization, Methodology, Software, Data Curation, Supervision, Funding Acquisition, Writing-original draft, Writing-review & editing;
Dora Hermes: Software, Formal Analysis, Supervision, Funding Acquisition, Writing-original draft, Writing-review & editing

Additional files

Data availability

To foster reproducible research, we will make the data and code publicly available upon final version via a permanent archive on the Open Science Framework and the code to reproduce the figure on Github.

References

Adrian ED, Matthews BH. The Berger rhythm: potential changes from the occipital lobes in man. Brain. 1934; 57(4):355–385. doi: 10.1093/brain/57.4.355.

Babu Henry Samuel I, Wang C, Hu Z, Ding M. The frequency of alpha oscillations: Task-dependent modulation and its functional significance. NeuroImage. 2018; 183:897–906. doi: 10.1016/j.neuroimage.2018.08.063.

Barbur J, Wolf J, Lennie P. Visual processing levels revealed by response latencies to changes in different visual attributes. Proceedings of the Royal Society of London Series B: Biological Sciences. 1998; 265(1412):2321–2325. doi: 10.1098/rspb.1998.0578.

Berger H. Über das elektroenkephalogramm des menschen. Archiv für psychiatrie und nervenkrankheiten. 1929; 87(1):527–570.

Bokil H, Andrews P, Kulkarni JE, Mehta S, Mitra PP. Chronux: A platform for analyzing neural signals. Journal of Neuroscience Methods. 2010; 192(1):146–151. doi: 10.1016/j.jneumeth.2010.06.020.

Bollimunta A, Mo J, Schroeder CE, Ding M. Neuronal mechanisms and attentional modulation of corticothalamic alpha oscillations. Journal of Neuroscience. 2011; 31(13):4935–4943. doi: 10.1523/JNEUROSCI.5580-10.2011.

Bonnefond M, Jensen O. The role of alpha oscillations in resisting distraction. Trends in Cognitive Sciences. 2024; doi: 10.1016/j.tics.2024.11.004.

Bullock D, Takemura H, Caiafa CF, Kitchell L, McPherson B, Caron B, Pestilli F. Associative white matter connecting the dorsal and ventral posterior human cortex. Brain structure and Function. 2019; 224:2631–2660. doi: 10.1007/s00429-019-01907-8.

Buracas GT, Boynton GM. The effect of spatial attention on contrast response functions in human visual cortex. Journal of Neuroscience. 2007; 27(1):93–97. doi: 10.1523/JNEUROSCI.3162-06.2007.

Capotosto P, Babiloni C, Romani GL, Corbetta M. Frontoparietal cortex controls spatial attention through modulation of anticipatory alpha rhythms. Journal of Neuroscience. 2009; 29(18):5863–5872. doi: 10.1523/JNEUROSCI.0539-09.2009.

Capotosto P, Babiloni C, Romani GL, Corbetta M. Differential contribution of right and left parietal cortex to the control of spatial attention: a simultaneous EEG–rTMS study. Cerebral cortex. 2012; 22(2):446–454. doi: 10.1093/cercor/bhr127.

Davidesco I, Harel M, Ramot M, Kramer U, Kipervasser S, Andelman F, Neufeld MY, Goelman G, Fried I, Malach R. Spatial and Object-Based Attention Modulates Broadband High-Frequency Responses across the Human Visual Cortical Hierarchy. Journal of Neuroscience. 2013; 33(3):1228–1240. doi: 10.1523/JNEUROSCI.3181-12.2013.

Desimone R, Duncan J, et al. Neural mechanisms of selective visual attention. Annual review of neuroscience. 1995; 18(1):193–222. doi: 10.1146/annurev.ne.18.030195.001205.

Distler C, Boussaoud D, Desimone R, Ungerleider LG. Cortical connections of inferior temporal area TEO in macaque monkeys. Journal of Comparative Neurology. 1993; 334(1):125–150. doi: 10.1002/cne.903340111.

Donoghue T, Schaworonkow N, Voytek B. Methodological considerations for studying neural oscillations. European journal of neuroscience. 2022; 55(11-12):3502–3527. doi: https://doi.org/10.1111/ejn.15361.

Felleman DJ, Van Essen DC. Distributed hierarchical processing in the primate cerebral cortex. Cerebral Cortex. 1991; 1(1):1–47. doi: 10.1093/cercor/1.1.1-a.

Giesbrecht B, Weissman DH, Woldorff MG, Mangun GR. Pre-target activity in visual cortex predicts behavioral performance on spatial and feature attention tasks. Brain research. 2006; 1080(1):63–72. doi: 10.1016/j.brainres.2005.09.068.

Gilbert CD, Li W. Top-down influences on visual processing. Nature reviews neuroscience. 2013; 14(5):350–363. doi: doi/10.1038/nrn3476.

Groen II, Piantoni G, Montenegro S, Flinker A, Devore S, Devinsky O, Doyle W, Dugan P, Friedman D, Ramsey NF, et al. Temporal dynamics of neural responses in human visual cortex. Journal of Neuroscience. 2022; 42(40):7562–7580. doi: 10.1523/JNEUROSCI.1812-21.2022.

Grotheer M, Jeska B, Grill-Spector K. A preference for mathematical processing outweighs the selectivity for Arabic numbers in the inferior temporal gyrus. NeuroImage. 2018; 175:188–200. doi: 10.1016/j.neuroimage.2018.03.064.

Halgren E, Wang C, Schomer DL, Knake S, Marinkovic K, Wu J, Ulbert I. Processing stages underlying word recognition in the anteroventral temporal lobe. Neuroimage. 2006; 30(4):1401–1413. doi: 10.1016/j.neuroimage.2005.10.053.

Hermes D, Miller K, Wandell B, Winawer J. Stimulus dependence of gamma oscillations in human visual cortex. Cerebral cortex. 2015; 25(9):2951–2959. doi: 10.1093/cercor/bhu091.

Hermes D, Nguyen M, Winawer J. Neuronal synchrony and the relation between the blood-oxygen-level dependent response and the local field potential. PLoS biology. 2017; 15(7):e2001461. doi: 10.1371/journal.pbio.2001461.

Hermes D, Petridou N, Kay KN, Winawer J. An image-computable model for the stimulus selectivity of gamma oscillations. Elife. 2019; 8:e47035. doi: https://doi.org/10.7554/eLife.47035.

Huk AC, Heeger DJ. Task-related modulation of visual cortex. Journal of neurophysiology. 2000; 83(6):3525–3536. doi: 10.1152/jn.2000.83.6.3525.

Jacques C, Witthoft N, Weiner KS, Foster BL, Rangarajan V, Hermes D, Miller KJ, Parvizi J, Grill-Spector K. Corresponding ECoG and fMRI category-selective signals in human ventral temporal cortex. Neuropsychologia. 2016; 83:14–28. doi: 10.1016/j.neuropsychologia.2015.07.024.

Jensen O, Mazaheri A. Shaping functional architecture by oscillatory alpha activity: gating by inhibition. Frontiers in human neuroscience. 2010; 4:186. doi: 10.3389/fnhum.2010.00186.

Kastner S, Pinsk MA, De Weerd P, Desimone R, Ungerleider LG. Increased activity in human visual cortex during directed attention in the absence of visual stimulation. Neuron. 1999; 22(4):751–761. doi: 10.1016/S0896-6273(00)80734-5.

Kay K, Bonnen K, Denison RN, Arcaro MJ, Barack DL. Tasks and their role in visual neuroscience. Neuron. 2023; doi: 10.1016/j.neuron.2023.03.022.

Kay KN, Weiner KS, Grill-Spector K. Attention reduces spatial uncertainty in human ventral temporal cortex. Current Biology. 2015; 25(5):595–600. doi: 10.1016/j.cub.2014.12.050.

Kay KN, Yeatman JD. Bottom-up and top-down computations in word-and face-selective cortex. elife. 2017; 6:e22341. doi: 10.7554/eLife.22341.

Luck SJ, Chelazzi L, Hillyard SA, Desimone R. Neural mechanisms of spatial selective attention in areas V1, V2, and V4 of macaque visual cortex. Journal of neurophysiology. 1997; 77(1):24–42. doi: 10.1152/jn.1997.77.1.24.

Manning JR, Jacobs J, Fried I, Kahana MJ. Broadband shifts in local field potential power spectra are correlated with single-neuron spiking in humans. Journal of Neuroscience. 2009; 29(43):13613–13620. doi: 10.1523/JNEUROSCI.2041-09.2009.

Maris E, Oostenveld R. Nonparametric statistical testing of EEG-and MEG-data. Journal of neuroscience methods. 2007; 164(1):177–190. doi: 10.1016/j.jneumeth.2007.03.024.

Markov NT, Ercsey-Ravasz MM, Ribeiro Gomes A, Lamy C, Magrou L, Vezoli J, Misery P, Falchier A, Quilodran R, Gariel MA, et al. A weighted and directed interareal connectivity matrix for macaque cerebral cortex. Cerebral cortex. 2014; 24(1):17–36. doi: 10.1093/cercor/bhs270.

Martin AB, Yang X, Saalmann YB, Wang L, Shestyuk A, Lin JJ, Parvizi J, Knight RT, Kastner S. Temporal dynamics and response modulation across the human visual system in a spatial attention task: an ECoG study. Journal of Neuroscience. 2019; 39(2):333–352. doi: 10.1523/JNEUROSCI.1889-18.2018.

McAdams CJ, Maunsell JH. Effects of attention on the reliability of individual neurons in monkey visual cortex. Neuron. 1999; 23(4):765–773. doi: 10.1016/S0896-6273(00)81206-4.

McDonald CR, Thesen T, Carlson C, Blumberg M, Girard HM, Trongnetrpunya A, Sherfey JS, Devinsky O, Kuzniecky R, Dolye WK, et al. Multimodal imaging of repetition priming: using fMRI, MEG, and intracranial EEG to reveal spatiotemporal profiles of word processing. Neuroimage. 2010; 53(2):707–717. doi: 10.1016/j.neuroimage.2010.06.069.

Miller KJ, Zanos S, Fetz EE, den Nijs M, Ojemann JG. Decoupling the Cortical Power Spectrum Reveals Real-Time Representation of Individual Finger Movements in Humans. Journal of Neuroscience. 2009; 29(10):3132–3137. doi: 10.1523/JNEUROSCI.5506-08.2009.

Miller KJ, Hermes D, Honey CJ, Hebb AO, Ramsey NF, Knight RT, Ojemann JG, Fetz EE. Human motor cortical activity is selectively phase-entrained on underlying rhythms. PLoS Computational Biology. 2012; doi: 10.1371/journal.pcbi.1002655.

Miller KJ, Honey CJ, Hermes D, Rao RP, Ojemann JG, et al. Broadband changes in the cortical surface potential track activation of functionally diverse neuronal populations. Neuroimage. 2014; 85:711–720. doi: 10.1016/j.neuroimage.2013.08.070.

Miller KJ, Sorensen LB, Ojemann JG, Den Nijs M. Power-law scaling in the brain surface electric potential. PLoS computational biology. 2009; 5(12):e1000609. doi: 10.1371/journal.pcbi.1000609.

Murray SO. The effects of spatial attention in early human visual cortex are stimulus independent. Journal of vision. 2008; 8(10):2–2. doi: 10.1167/8.10.2.

Ogawa T, Komatsu H. Target selection in area V4 during a multidimensional visual search task. Journal of Neuroscience. 2004; 24(28):6371–6382. doi: 10.1523/JNEUROSCI.0569-04.2004.

Osaka M. Peak alpha frequency of EEG during a mental task: Task difficulty and hemispheric differences. Psychophysiology. 1984; 21(1):101–105. doi: 10.1111/j.1469-8986.1984.tb02325.x.

Panesar SS, Belo JTA, Yeh FC, Fernandez-Miranda JC. Structure, asymmetry, and connectivity of the human temporo-parietal aslant and vertical occipital fasciculi. Brain Structure and Function. 2019; 224:907–923. doi: 10.1007/s00429-018-1812-0.

Pins D, Bonnet C. On the relation between stimulus intensity and processing time: Piéron's law and choice reaction time. Perception & psychophysics. 1996; 58:390–400. doi: 10.3758/BF03206815.

Plainis S, Murray I. Neurophysiological interpretation of human visual reaction times: effect of contrast, spatial frequency and luminance. Neuropsychologia. 2000; 38(12):1555–1564. doi: 10.1016/S0028-3932(00)00100-7.

Rajagovindan R, Ding M. From prestimulus alpha oscillation to visual-evoked response: an inverted-U function and its attentional modulation. Journal of cognitive neuroscience. 2011; 23(6):1379–1394. doi: 10.1162/jocn.2010.21478.

Ray S, Maunsell JH. Different origins of gamma rhythm and high-gamma activity in macaque visual cortex. PLoS biology. 2011; 9(4):e1000610. doi: 10.1371/journal.pbio.1000610.

Ray WJ, Cole HW. EEG alpha activity reflects attentional demands, and beta activity reflects emotional and cognitive processes. Science. 1985; 228(4700):750–752. doi: 10.1126/science.3992243.

Ress D, Backus BT, Heeger DJ. Activity in primary visual cortex predicts performance in a visual detection task. Nature neuroscience. 2000; 3(9):940–945. doi: 10.1038/78856.

Reynolds JH, Pasternak T, Desimone R. Attention increases sensitivity of V4 neurons. Neuron. 2000; 26(3):703–714. doi: 10.1016/S0896-6273(00)81206-4.

Saalmann YB, Pinsk MA, Wang L, Li X, Kastner S. The pulvinar regulates information transmission between cortical areas based on attention demands. science. 2012; 337(6095):753–756. doi: 10.1126/science.1223082.

Sabra Z, Bonilha L, Naselaris T. Spectral encoding of seen and attended object categories in the human brain. Journal of Neuroscience. 2020; 40(2):327–342. doi: 10.1523/JNEUROSCI.0900-19.2019.

Schalk G. A general framework for dynamic cortical function: the function-through-biased-oscillations (FBO) hypothesis. Frontiers in Human Neuroscience. 2015; 9. doi: 10.3389/fnhum.2015.00352.

Silvanto J, Muggleton N, Lavie N, Walsh V. The perceptual and functional consequences of parietal top-down modulation on the visual cortex. Cerebral Cortex. 2009; 19(2):327–330. doi: 10.1093/cercor/bhn091.

Silver MA, Ress D, Heeger DJ. Neural Correlates of Sustained Spatial Attention in Human Early Visual Cortex. Journal of Neurophysiology. 2007; 97(1):229–237. doi: 10.1152/jn.00677.2006.

Takemura H, Rokem A, Winawer J, Yeatman JD, Wandell BA, Pestilli F. A major human white matter pathway between dorsal and ventral visual cortex. Cerebral cortex. 2016; 26(5):2205–2214. doi: 10.1093/cercor/bhv064.

Vinci-Booher S, Caron B, Bullock D, James K, Pestilli F. Development of white matter tracts between and within the dorsal and ventral streams. Brain Structure and Function. 2022; 227(4):1457–1477. doi: 10.1007/s00429-021-02414-5.

Webster MJ, Bachevalier J, Ungerleider LG. Connections of inferior temporal areas TEO and TE with parietal and frontal cortex in macaque monkeys. Cerebral cortex. 1994; 4(5):470–483. doi: 10.1093/cercor/4.5.470.

Yantis S, Schwarzbach J, Serences JT, Carlson RL, Steinmetz MA, Pekar JJ, Courtney SM. Transient neural activity in human parietal cortex during spatial attention shifts. Nature neuroscience. 2002; 5(10):995–1002. doi: 10.1038/nn921.

Yeatman JD, Weiner KS, Pestilli F, Rokem A, Mezer A, Wandell BA. The vertical occipital fasciculus: a century of controversy resolved by in vivo measurements. Proceedings of the National Academy of Sciences. 2014; 111(48):E5214–E5223. doi: 10.1073/pnas.141850311.

Yuasa K, Groen IIA, Piantoni G, Montenegro S, Flinker A, Devore S, Devinsky O, Doyle W, Dugan P, Friedman D, Ramsey N, Petridou N, Winawer J. Precise Spatial Tuning of Visually Driven Alpha Oscillations in Human Visual Cortex. bioRxiv. 2023; doi: 10.1101/2023.02.11.528137.

Zhang RY, Kay K. Flexible top-down modulation in human ventral temporal cortex. Neuroimage. 2020; 218:116964. doi: 10.1016/j.neuroimage.2020.116964.

Zhigalov A, Jensen O. Alpha oscillations do not implement gain control in early visual cortex but rather gating in parieto-occipital regions. Human Brain Mapping. 2020; 41(18):5176–5186. doi: 10.1002/hbm.25183.

Zhou J, Benson NC, Kay K, Winawer J. Predicting neuronal dynamics with a delayed gain control model. PLoS computational biology. 2019; 15(11):e1007484. doi: 10.1371/journal.pcbi.1007484.

Zhou J, Benson NC, Kay KN, Winawer J. Compressive temporal summation in human visual cortex. Journal of Neuroscience. 2018; 38(3):691–709. doi: 10.1523/JNEUROSCI.1724-17.2017.

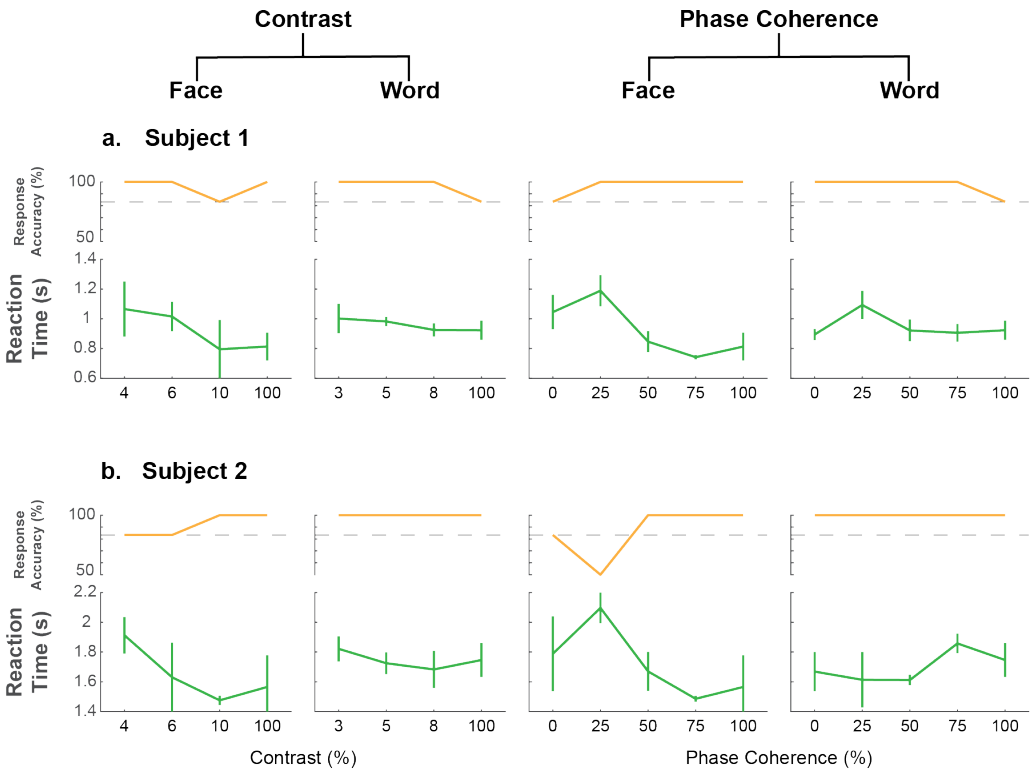

Figure 1—figure supplement 1. Behavioral response during categorization task. Button press responses for (a) Subject 1 and (b) Subject 2. The top plot for each subject shows the response accuracy in percentage. The bottom plot shows the average reaction time (median across trials) in s. Error bars indicate 68% CI. The dashed line in top plots indicate 83.33% accuracy (5 of 6 correct responses).

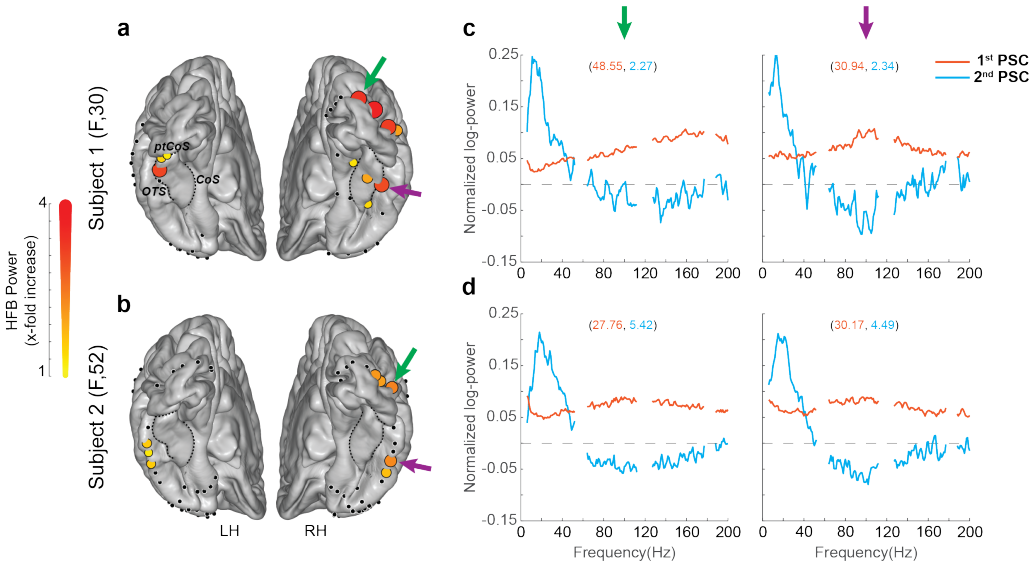

641

Figure 2—figure supplement 1. Power spectral components. (a,b) ECoG electrode locations in subject 1 (top) and subject 2 (bottom). Visual-responsive electrodes are shown in colored circles; color and size of the circle indicates the intensity of time-averaged HFB power increase (0-400 ms, face & word responses at 100% contrast). (c,d) First two PSCs for an EVC electrode (green arrow) and a VTC electrode (purple arrow) in each subject. The numbers in the parentheses denote the percent variance explained by each of the two PSCs. *COS*: collateral sulcus, *ptCOS*: posterior transverse COS, *OTS*: occipital-temporal sulcus

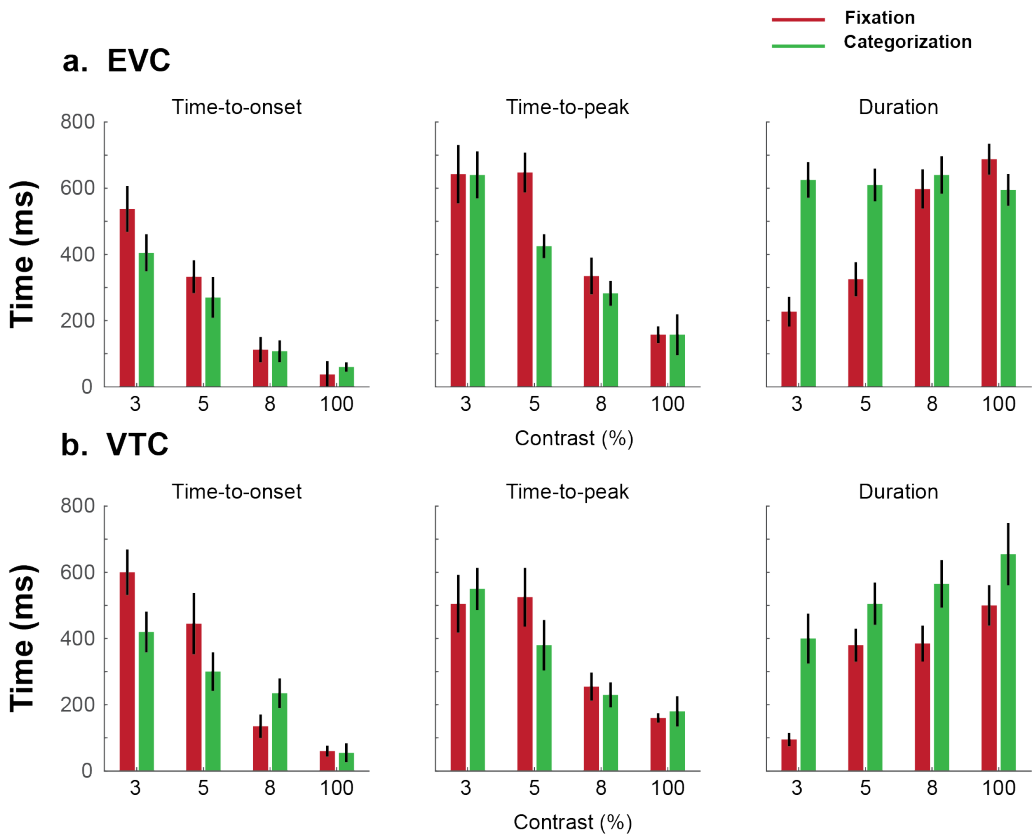

Figure 4—figure supplement 1. Temporal characteristics of HFB power increases. Time-to-onset (left), time-to-peak (center), and significant response duration (right) shown for (a) EVC and (b) VTC electrodes. Responses for each condition were combined for faces and words for EVC electrodes. For VTC electrodes, responses per condition were combined only for the selective electrodes (i.e., faces from FFA electrodes and words from vWFA electrodes). Verticals bars indicate 68% confidence interval.

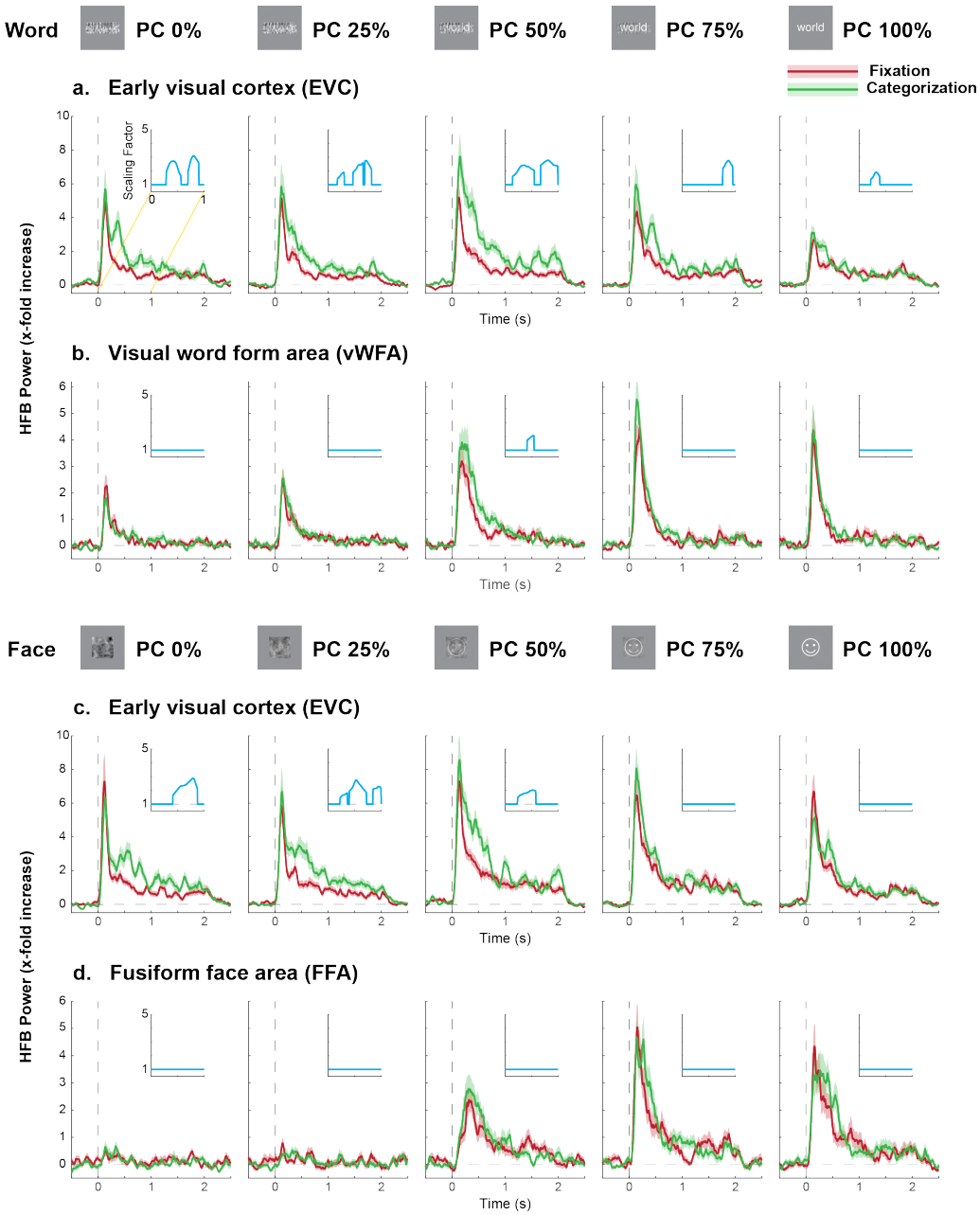

Figure 4—figure supplement 2. HFB power increases during phase coherence variation. Same as ***Figure 4***, except for increasing stimulus phase coherence instead.

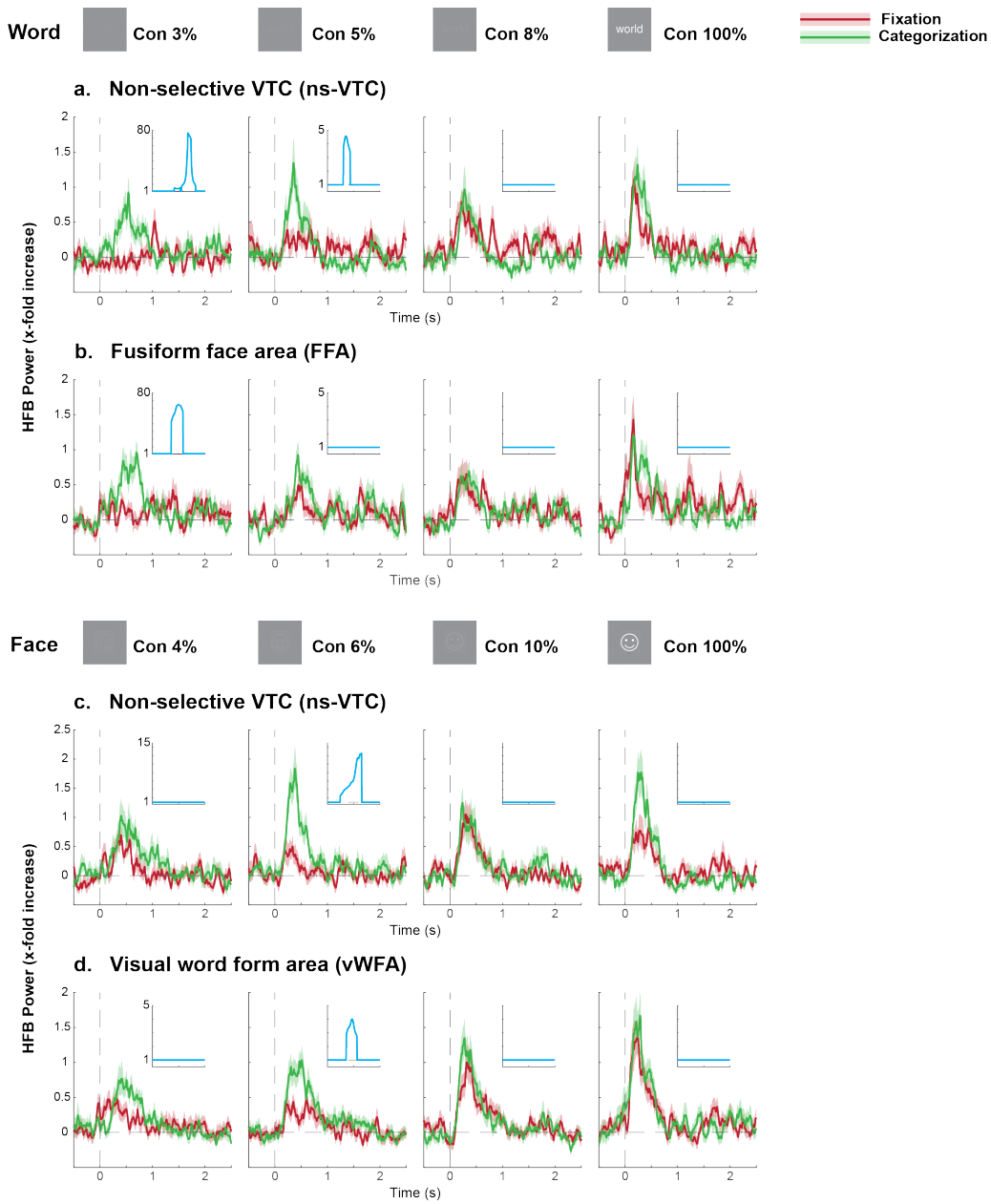

Figure 4—figure supplement 3. HFB power increases during contrast variation (non-selective electrodes). Same as ***Figure 4*** (a,b) HFB power for increasing word contrast in ns-VTC and FFA. (c,d) HFB power for increasing face contrast in ns-VTC and vWFA.

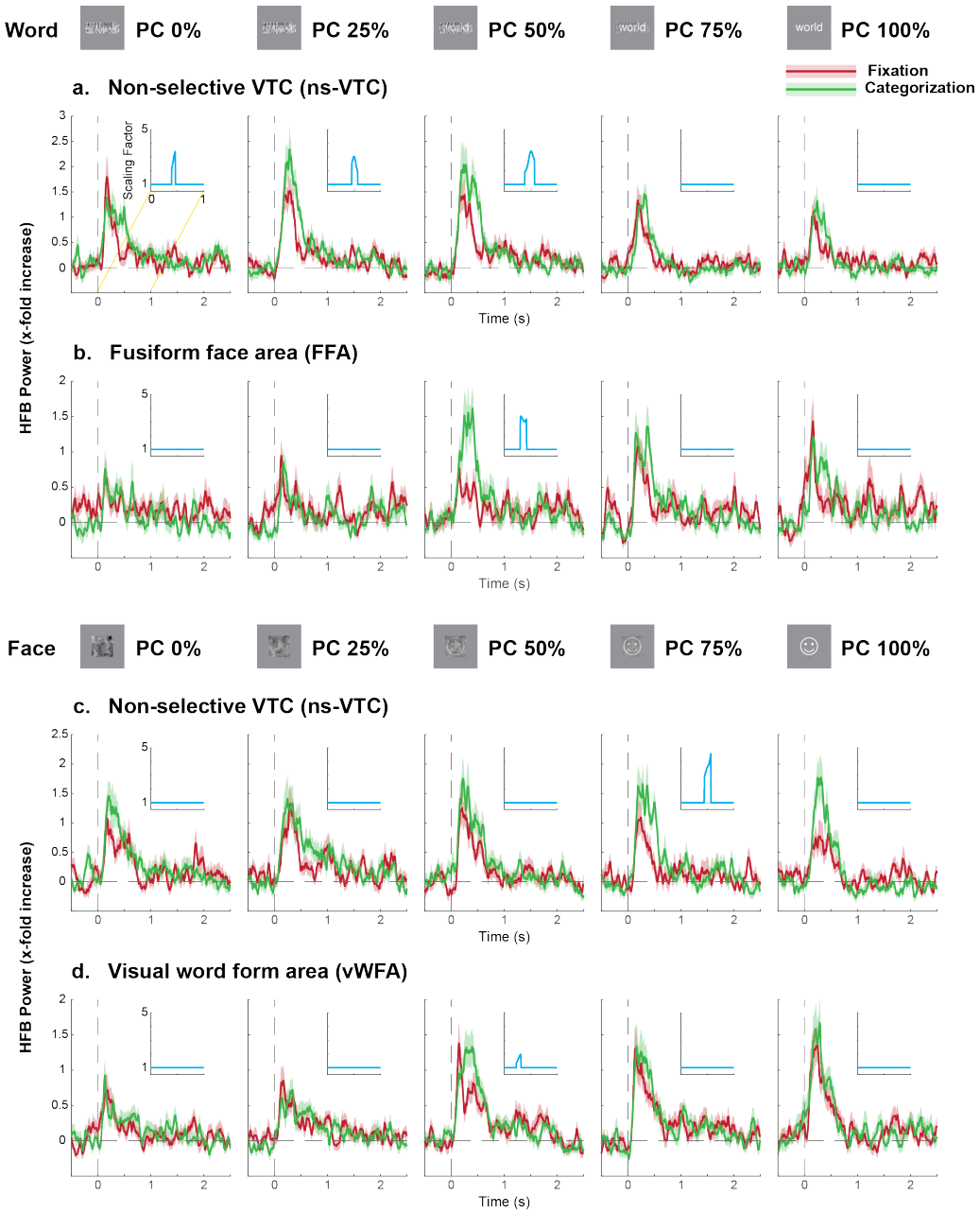

Figure 4—figure supplement 4. HFB power increases during phase coherence variation (non-selective electrodes). Same as ***Figure 4—figure Supplement 2*** (a,b) HFB power for increasing word contrast in ns-VTC and FFA. (c,d) HFB power for increasing face contrast in ns-VTC and vWFA.

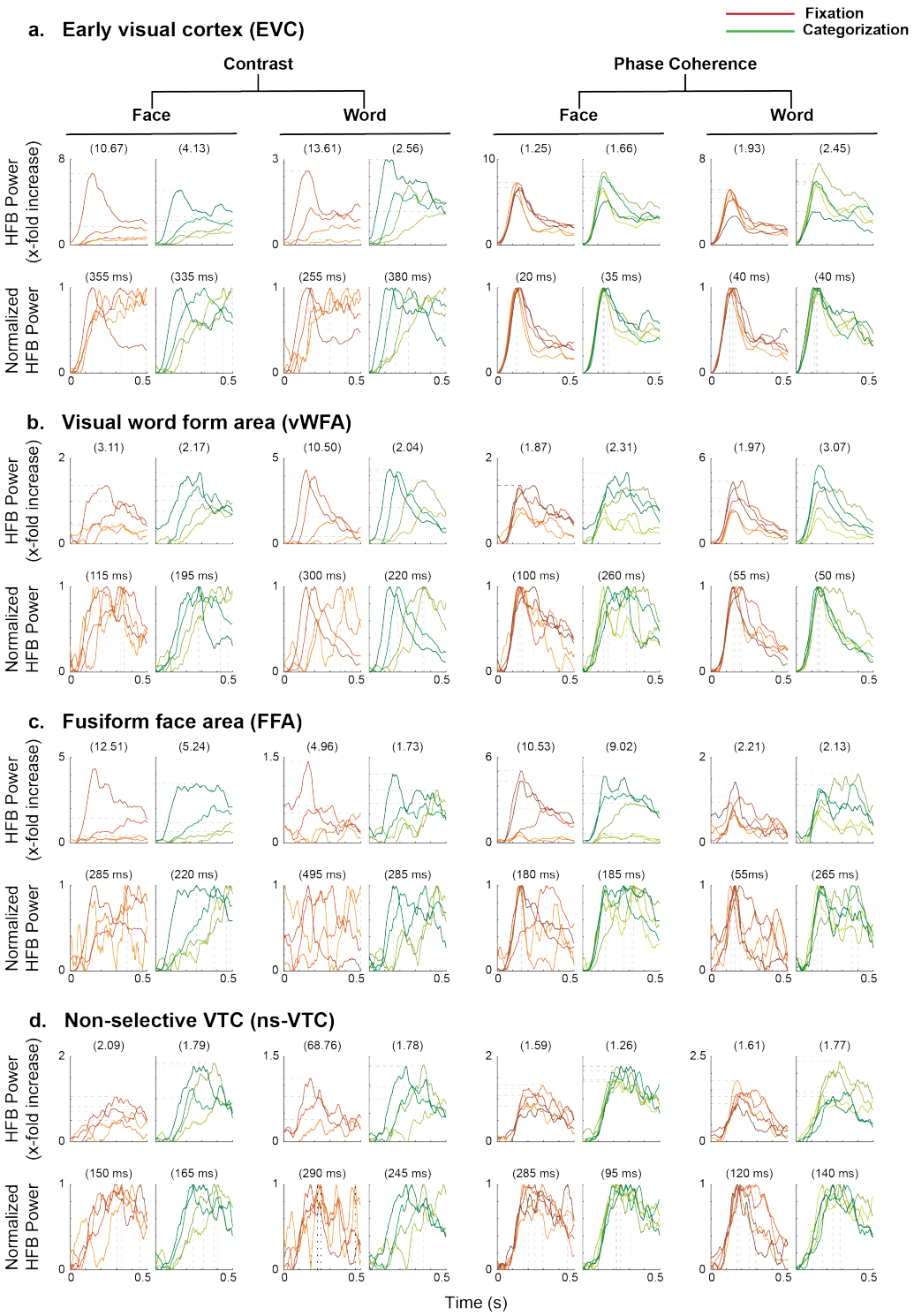

Figure 4—figure supplement 5. Summary plots of HFB power increases across stimulus manipulation. Top plots show average HFB power increases from 0 - 0.5 s for increasing contrast / phase coherence. The number in the parentheses indicate ratio of the peak HFB power (horizontal dashed lines) for the highest to the lowest contrast / phase coherence. Bottom plots show the normalized power. The number in the parentheses indicate the difference in the time to peak (vertical dashed lines) between the highest to the lowest contrast / phase coherence. Darker shades indicate higher contrast / phase coherence.

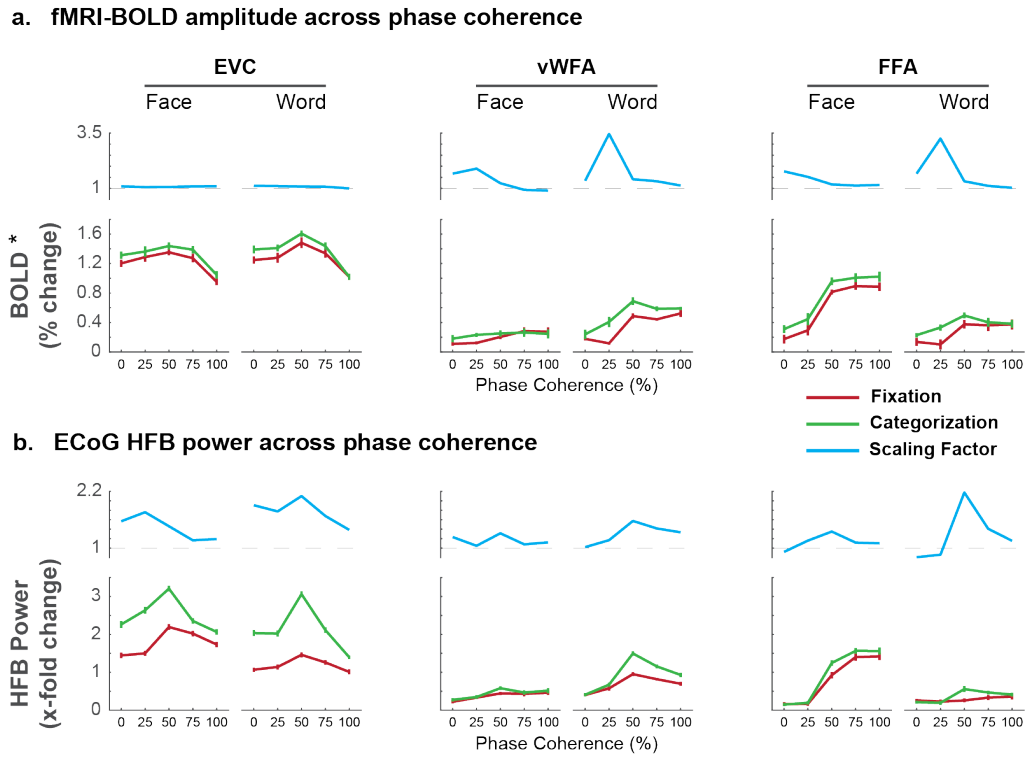

Figure 5—figure supplement 1. Time-averaged ECoG HFB responses match fMRI BOLD amplitudes for phase coherence manipulations. Same as ***Figure 5***, except for variations across stimulus phase coherence instead.

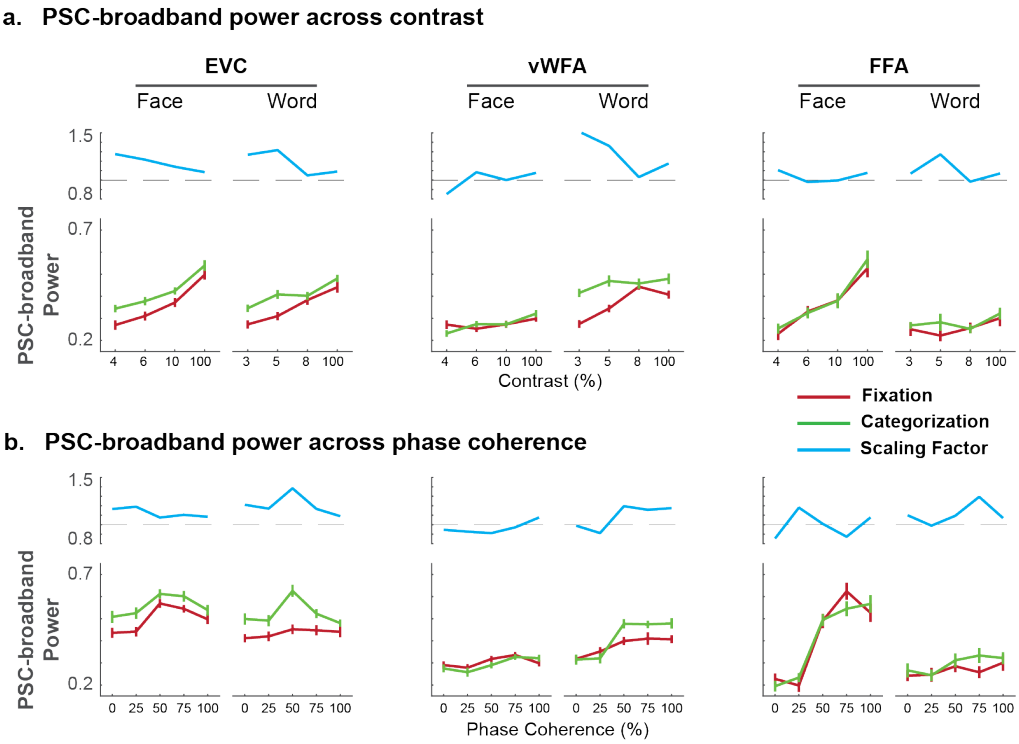

Figure 5—figure supplement 2. PSC-based HFB responses for contrast and phase coherence manipulations. HFB responses computed for varying stimulus (a) contrast and (b) phase coherence based on the first spectral PCA for EVC (left) vWFA (middle) and FFA (right) and time-averaged in 0-1 s time window. (b) Cyan traces show scaling factors with horizontal dashed line at 1 indicating no scaling.

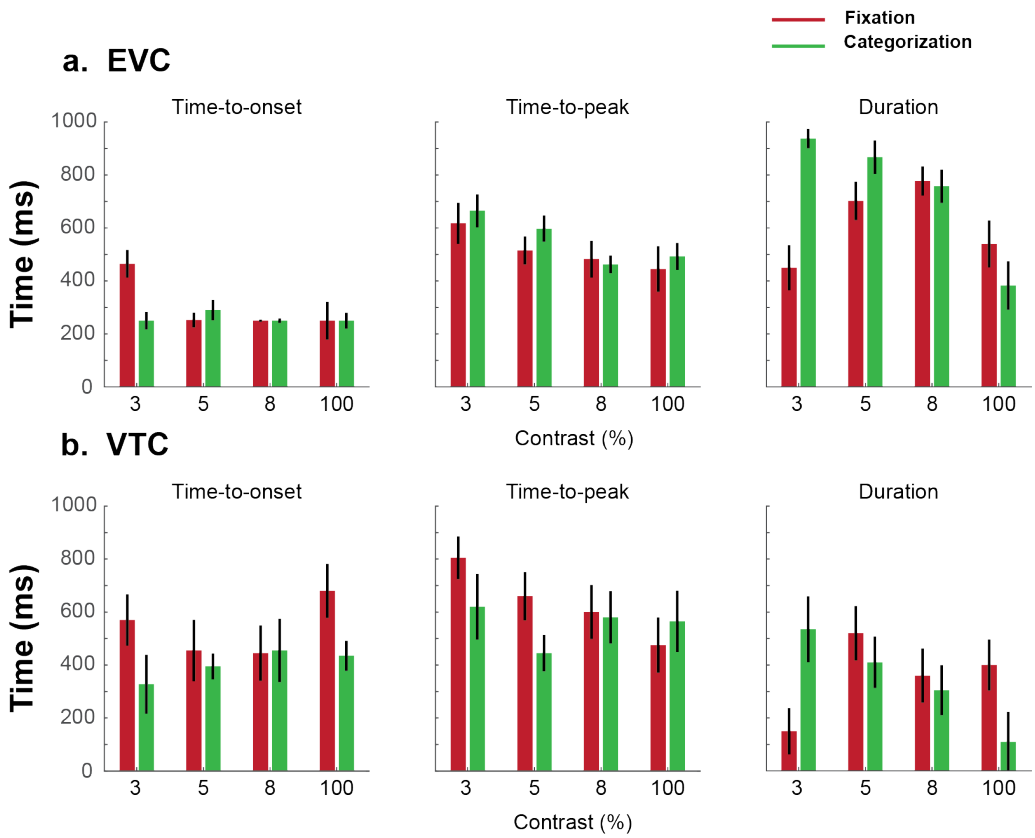

Figure 6—figure supplement 1. Temporal characteristics of LFB power suppression. Time-to-onset (left), time-to-peak suppression (center), and significant response duration (right) shown for (a) EVC and (b) VTC electrodes. Responses for each condition were combined for faces and words for EVC electrodes. For VTC electrodes, responses per condition were combined only for the selective electrodes (i.e., faces from FFA electrodes and words from vWFA electrodes). Verticals bars indicate 68% confidence interval.

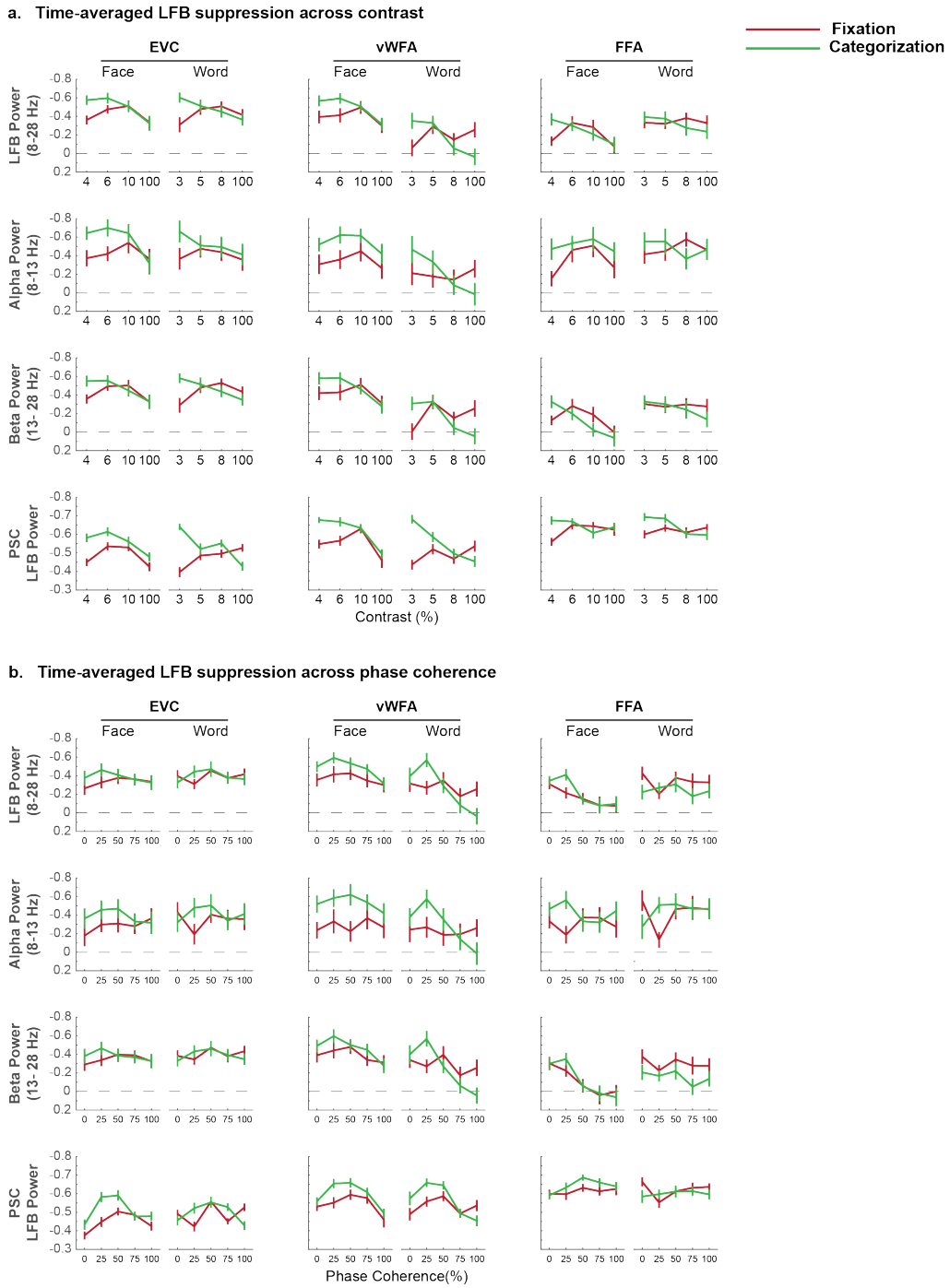

Figure 6—figure supplement 2. Time-averaged ECoG LFB suppression across different conditions. (a) ECoG responses time-averaged in 0.25-1.25 s time window using filtering in LFB (8-28 Hz; top), alpha (8-13 Hz, mid-top), and beta (13-18 Hz, mid-bottom) frequencies, and using second spectral PCA (bottom). Verticals bars indicate 68% confidence interval. (b) Same as (a), except for variations across stimulus phase coherence instead.